

We thank both reviewers for their supportive and thorough review, and acknowledge all of the points made. Most of the comments concern the presentation and the discussion of the results. We agree on that and aim to better present the results in a revised version of the manuscript. We highly appreciate the suggestions and follow most of the comments to provide a better and self-contained manuscript so that the purpose of the research and results become much clearer.

Due to the comments, the revised version of the manuscript will have the following major changes:

- The second part of the Introduction is rewritten. A major consequence is that the main focus of the paper is now on the grid dependency. We dropped the (secondary) aim to present the AWI-ISSM model in detail. So, we still present more details of AWI-ISSM compared to Goelzer et al (2020), but we put more weight on the grid-dependence.
- The *Discussion* is improved. We identified paragraphs in the *Results* section, which should belong to the *Discussion* (this might have also confused the reviewers - apologies). We moved them accordingly. The original paragraphs were found on page 14, line 320-323; page 16, line 353-364 and on page 17, line 378-383 in the first version of the manuscript, see point-to-point answers below.
- We have added a new subsection focussing on the comparability of the experiments.
- As requested by the reviewers, we re-structured the description of the ISM used and description of the experiments. With that, we hope to gather all information in the appropriate sections. The structure now looks as:

- 2. Methods and experiments
 - 2.1 Ice flow model ISSM
 - 2.2 Overview of experiments
 - 2.3 Initialization experiment
 - 2.4 Historical experiment
 - 2.5 Future forcing experiments
 - 2.5.1 Atmospheric forcing
 - 2.5.2 Oceanic forcing
 - 2.6 Comparability of experiments (**new**)

We reply to each point made (reviewer text = black text) below using blue text. The changes to the manuscript will be found at the end of the responses to the reviewer comments.

==== Reviewer 1 =====

General comments: The ISMIP6 project is an important effort towards improving projections of the contribution to global sea level rise from the large ice sheets in Greenland and Antarctica. This paper by Rückamp et al. presents result from a particular model from the ISMIP6 project. They show that the projected SLR is sensitive to the spatial resolution in their model, and they show further that the effect depends on the climate forcing, with oceanic and atmospheric forcings showing opposite and non-trivial responses. Investigations of how ice flow modelling techniques and model parameters influence the projected SLR and

the uncertainties is highly relevant and very important, and the main conclusions of this paper are interesting and merits publication. While the scientific quality of the modelling work is high, the presentation and text are not at the same level. As a result, the purpose of the paper is not clear, the text needs to be edited and self-contained, and the conclusions could be more clearly communicated and supported by the text. The paper appears to be hastily written. Furthermore, the important relation between the resolution of the bedrock topography and the model resolution is not sufficiently discussed.

We would like to thank the reviewer for his/her generally positive evaluation. The comments are very helpful to clean the previous version of the manuscript and provide a better and concise story.

Here are some important issues:

1. The purpose of the paper is mixed and not clear. I recommend that the authors focus on investigating the influence from the spatial resolution and the different effects on oceanic and atmospheric forcings. Please be sure to structure the text to emphasize this purpose.

We have restructured the text , i.e. experiment description and aim of paper, as outlined above. We believe with restructuring the text, that the purpose of the paper to investigate the influence from the spatial resolution on future forcing experiments is now more highlighted.

Remove the secondary aim, i.e. to describe how the ISSM-AWI contributed to the ISMIP6 exercise. This is out of scope here, unless necessary to understand the results of this paper, and should then be part of the methods section.

You are right, we deleted all unnecessary information e.g. how AWI-ISSM contributed to ISMIP6. In doing so, we now emphasize the grid-dependency as major aim.

Rewrite the last sections of the introduction to reflect this. The current version seems unclear, particularly the last paragraph, lines 85-91.

To emphasize the focus of the paper, we modified the last paragraph of the *Introduction* (Lines 73-81 in the new version of the manuscript).

2. The introduction starts out being very general and later becomes very specific. Shorten the details of the work by Aschwanden et al., they seem to be too detailed for the introduction.

We agree that there are too many details in the *Introduction*. We have shortened and reorganized the material in the second part of the *Introduction*.

3. Remove all the additional comments about how the ISSM-AWI model contributed to the ISMIP6 project, e.g. lines 127-126, and several paragraphs in section 2. I don't think that this really supports the conclusions of the paper.

We have reorganized the material and focus on the grid-dependency.

4. Again, comments about how the ISSM-AWI model is set up must be presented in a self-contained way in this paper, so please rewrite section 2, and avoid structuring the text as an appendix to the paper by Goelzer et al. Also, remove the first sentence of section

3.3.2, as well as providing details of the ISMIP6 AWI-ISSM6 simulation, which is not reported in this paper. Also, change figure 2 to show results from a run presented here, and not from a G8000 run, which was not reported.

We completely rearranged the material to present a better and self-contained story.

Not exactly sure what you mean with AWI-ISSM6, as it does not appear in the manuscript.

We think the comment refers to AWI-ISSM1? If so, the reference to AWI-ISSM1 is deleted.

“G8000” was a typo and now changed to “G4000”.

5. The inversion parameters are not discussed in detail, and neither their influence on the simulated velocity field, e.g. how the regularization term smooth out sharp transitions in sliding (in order to avoid oscillations). How does this relate to the spatial resolution, and how sensitive are the results to the regularization parameters?

We have not explored in depth how the parameters will change across the different spatial resolutions. To find the optimal inversion parameters, we need to run an L-curve analysis for each grid. For a high-resolution setup this was already done by Seroussi et al. (2013) and we adopt these parameters (see page 8, line 181). To run an L-curve analysis for the coarser resolutions is beyond the scope of this study. In fact, we wanted to keep all parameters similar and argue that the simulations should therefore be comparable (for the same reason, we do not induce a SMB correction to minimize the drift in the control run). We added a section “Comparability of experiments” to highlight our approach (Lines 232-244 in the new version of the manuscript). Additionally, we refer in the *Discussion* to this issue (Lines 469-476 in the new version of the manuscript).

6. The connection between the spatial resolution of the model and the ability to resolve bedrock topography should be highlighted more. This work shows that the results converge when the resolution is improved. But is the convergence just because the model resolution approaches the resolution of the bedrock topography map? Would the model results be different if finer resolution bedrock data were available? These are important questions, and they should be discussed in the paper, even if they cannot be fully addressed. In my opinion, the importance of high resolution bedrock data and the relation to the projected SLR is the most important contribution of this paper. Please make this come out more clearly.

We extended the discussion on page 18, line 425 between the spatial resolution of the model and the ability to resolve bedrock topography. Also we moved the paragraph from page 17, line 378-383 to the discussion. This paragraph particularly addresses one of your questions. We discussed a setup that adopted a high-resolution grid (G1000), but uses input data (e.g. bedrock) from a coarse resolution (G4000). This scenario shows a sea-level contribution that is closer to the G4000 simulation. This setup highlights that the response is highly dependent on how the bedrock is resolved. We believe by extending and restructuring the discussion, we have made this much clearer (Lines 392-432 and 438-450 in the new version of the manuscript).

7. Throughout the paper: the use of the word “dynamic” is not consistent. Dynamic is used to describe dynamic response, i.e. ice-dynamic changes due to ocean forcing, or dynamic residual, i.e. corrected for front retreat, and sometimes used more generally to describe ice dynamics. Perhaps use the word “discharge” when relevant to avoid confusion.

You are right, at some instances the use of “dynamic” was not consistent. We have corrected where necessary.

8. There are numerous errors in the use of English, e.g. proper instead of properly.
We have carefully read the manuscript and corrected the use of English where necessary.

A few specific points:

- The effective pressure, line 108: is this used generally, i.e. also in interior areas with bedrock below sea level?

Yes, we do not make a separation if areas are in contact with the ocean or not. The parametrization accounts for full water-pressure support from the ocean wherever the ice sheet base is below sea-level, even far into its interior where such a drainage system may not exist. We acknowledge, that this is a strong simplification of the model but an additional hydrological model would be needed to realistically simulate the effective basal pressure. We clarified it in the new version and add a paragraph in the discussion (Lines 461-468 in the new version of the manuscript).

- Regarding the inversion, please reference the remote sensing velocity product (it is not clear which product is used).

Indeed, there was a citing error. We changed Joughin et al. (2010) to Joughin et al. (2018) as requested by NSIDC (<https://nsidc.org/data/NSIDC-0670/versions/1>) for citing *MEaSURES Multi-year Greenland Ice Sheet Velocity Mosaic, Version 1*.

- Fig 3b – it is very difficult to see the colored areas. Please modify, e.g. change the black color of grounded ice to white, and remove all black outlines.

We have modified the colors. Instead of the showing the mask for the whole GrIS, we show only a subset.

- Section 4 first paragraph: provide units of the q and Q .

Done

- Figures S1+2: confusing caption: difference of a to b, what does that mean – $b-a$ or $a-b$? please clarify. (difference between a and b is $a-b$).

Done.

===== Reviewer 2 =====

This paper uses the ISSM model and the ISMIP6 protocol in order to investigate the importance of resolving the ice dynamics and the bed topography in Greenland ice sheet simulations. It does so by forcing ISSM using ocean-only retreat, SMB-only perturbations, and the combination of both ocean retreat and SMB perturbations. The paper concludes on the importance of model resolution with respect to the different forcing and how the bed topography resolution can be the ultimate limiting factor on how to choose adequate resolution for model predictions. The findings of this papers are of high quality and highly relevant for improving future projections from ice sheet models. I would highly support the publication of this paper after revisions suggested thereafter.

Thank you very much for the positive evaluation. Your detailed comments below are highly appreciated to improve the presentation of the manuscript. In most instances we followed your suggestions. A few suggestions arised from a misleading presentation in the first version of the manuscript, therefore we have not adopted them but clarified the presentation. The suggestion in comment 7, we have realized to that extent that we have polished the *Discussion*.

General comments:

1. The paper feels that it was written in a hurry, lacks clarity (especially before section 4.2), and could be better organized. There is too much of a focus on ISMIP6 and how the model used here participated in this effort. The paper could simply mention that it extends ISMIP6 contribution by deepening the analysis on the impact of forcing on the model and bed resolution and leave it at that. It is useful to provide a quick summary of the ISMIP6 experimental protocol since it is used as experimental design in the paper but there is no need to add all these references to ISMIP6 throughout the text. I found model descriptions in many different sections while they should be gathered in one place.

In the updated manuscript, we shortened the description of the ISMIP6 protocol and tried to group this type of information. The restructuring was also requested by Reviewer 1 (see his/her comments 1,3 and 4).

Similarly, the initialization technics and results should be discussed in a single section with more figures comparing to observations.

Reviewer 1 recommended dropping the AWI-ISSM details as one of the aims of the paper to make the grid sensitivity much clearer. As we followed his/her suggestion we decided that we will not present the performance of the initialization in detail. However, we updated the histogram plots in Fig. 4 by showing the RMSE values of the initialization. The text is updated accordingly. Additionally we added new figures to the supplement (Figs. S1, S2 and S3).

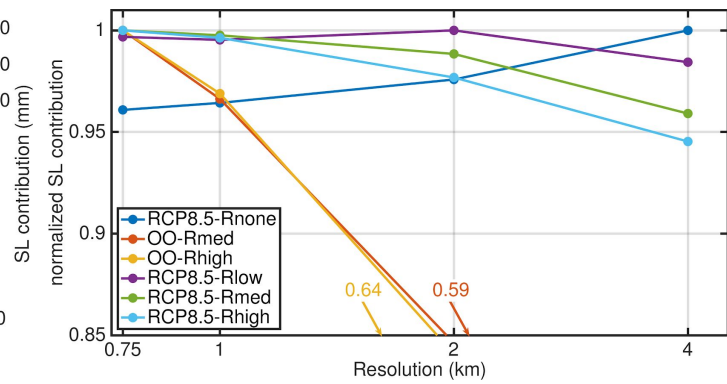
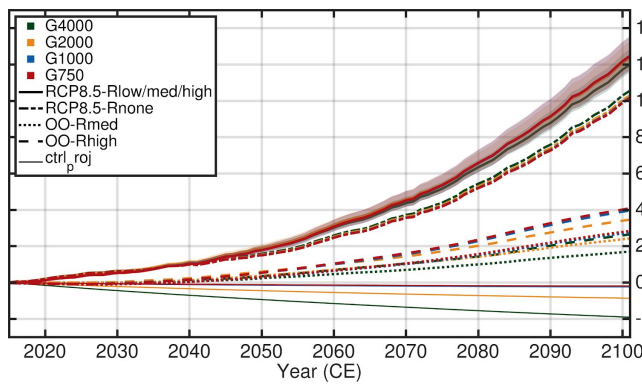
Terms are misused throughout the text.

We have carefully read the manuscript and corrected terms where necessary.

In the ISMIP6 protocol, what is called "Initial State" in section 4.1 is really the historical run. Indeed, we renamed section 4.1 "Initial state" to "Historical experiment".

The control experiment is relative to the state of the initial condition prior to running the historical experiment. The projection control is the one that should be performed starting from the end of the historical run until year 2100 and used in the result analysis section (instead of the control run). It does not appear in the paper and should be added.

In the revised version of the manuscript we define additionally the ctrl_proj experiment, similar as in Goelzer et al. (2020). When correcting the projections with ctrl_proj the magnitude of the SL contributions in 2100 of each experiment changes, but not the general behaviour (illustrated in the Figures above; equivalent to Figs. 5 and 7 in the manuscript but corrected with ctrl_proj). We added a table that lists all SL contributions from each



experiment corrected with both ctrl and ctrl_proj. However, in the revised version the results of sea-level contribution (Figs. 5 and 7) are still corrected with the ctrl run.

2. This paper is very good in discussing and analyzing the results on the model resolution dependence versus the use of grid resolution. It would be of even higher quality if it improved the analysis and the discussion of the dependence with respect to the bed topography versus model resolution (after all, it is major result here).

We have done this and described it in our answer to comment 6 of Reviewer 1.

3. The introduction tries to make a point on the importance of using an adequate resolution for modeling GrIS. However, this is only apparent towards the end of the introduction. It is difficult to follow why it was necessary to read the different paragraphs about iniMIP, Greve and Hertzfeld, Aschwanden 2016 and 2019, as no direct conclusions from these finding would lead to the thesis of this study. In particular the paper mentions that the resolution in Greve and Hertzfeld was too coarse to expect any better quantitative results (on top of using SIA). The introduction continues with describing Aschwanden's work that actually did use very high resolution with no real benefit over coarse resolution. At that point, I would expect a discussion of why that is and what this study will do differently.

The intention of describing iniMIP, Greve & Hertzfeld 2013, and Aschwanden et al. (2016,2019) was to outline the importance of the horizontal grid-resolution and outlining what is known about the grid-dependency on GrIS projections. We agree that we present too many details which are not necessary at this stage. We have now shortened the description and mention very briefly, that (1) the observed grid-dependency in iniMIP must be treated with some caution due to the methodological approach and that (2) in Greve & Hertzfeld (2013) and Aschwanden et al. (2019) no clear conclusion how the resolution affects the mass loss was found. From here we deduce one research question, that a separation of both forcings (atmosphere and ocean) must be considered to investigate the different responses (Lines 56-61 in the new version of the manuscript).

4. The initialization techniques lack clarity and details. The inversion parameters and their variations with model resolutions are not discussed.

We improved this considerably. Please see answer to comment 5 of Reviewer 1.

After the inversion, is the model run long enough to bring it to a steady state? If so for how long?

After the inversion we directly started the historical run. We don't perform any further relaxation run to bring the model to a steady-state. It is always a compromise between matching the observed geometry and being closer to a steady-state. Here, we put more weight on having the initial geometry closer to the observed geometry. This decision is-line with our approach having all parameters, parameterizations and inputs for all grids as similar as possible for a better comparison between the resolutions. As the model is not in steady-state at the initial state, we expect a model drift in the transient runs; which would not be the case for models that do a relaxation towards a steady-state after the inversion. To demonstrate the grid-dependent drift, we show the spatial patterns in Fig. (6).

We added: *“All transient simulations start from the initial state, that means, we do not perform a subsequent relaxation run to bring the model to a steady-state. We put more weight on having the geometry closer to the observed geometry for a better comparison between the resolutions.”*

What dataset (climatology, geothermal heat flux, ...) is used for the initialization?

Geothermal flux data set is mentioned on page 8 line 175. However, we would like to clarify that there is no thermo-mechanical coupling in the transient runs. Furthermore, no climatology/geothermal flux is used in our initialization approach. With the temperature field recovered from Rückamp et al. (2019) we just initialize the viscosity with a realistic temperature distribution rather than choosing e.g. a constant temperature (which is often done in inversion approaches). If climatology refers to which SMB product is used, that is outlined very detailed in section 3.3.1.

Is there a specific procedure (if any) initiated once the parameters are set? Please add more details on that topic. How are ice shelves constrained during the initialization? A figure highlighting how well the initialized ice sheet matches target observations would be a good addition (the authors mention they want this paper to describe in greater depth how the initialization was performed which could not be done in the ISMIP6 paper by Goelzer et al. 2020).

Our initialization procedure is based on data assimilation. That means we leverage BedMachine as geometric input and MEASURE velocities as target for the inversion method. Instead of showing the performance of the initialization ($v_{\text{simulated}}$ vs. v_{observed} and $\text{thickness}_{\text{simulated}}$ vs $\text{thickness}_{\text{observed}}$), we present the quality at the end of the historical run (Fig. 4). As the historical run causes some geometrical changes and velocity responses (as response to the imbalance of ice sheet which is not in equilibrium with the applied SMB and ice flux divergence), the misfits are a bit larger than directly after the initialization.

As we focused now more on the grid-dependency rather than on model description (as suggested by Reviewer 1), we tried to keep the description of the initialization procedure as briefly as possible. However, we slightly rewrote the initialization procedure to clarify certain aspects. Due to dropping the focus of the paper to present the AWI-ISSM details, we decided that we will not present the performance of the initialization in detail. However, we updated the histogram plots in Fig. 4 by showing the RMSE values of the initialization. Text is updated accordingly. Additionally we added new figures to the supplement (Figs. S1, S2 and S3).

5. The logic behind not using a sub-grid scheme to simulate fractional retreat in section 3.3.2 does not make sense to me. The argument that it might mimic a higher resolution is not sound as it is something already done for grounding line dynamics.

Our intention was to highlight that the coarser resolution models requesting a sub-grid scheme for the retreat according to the ISMIP6 protocol. The fractional retreat then mimics a higher resolution what we do not want here because the coarser models must rely on the parameters, parameterizations, inputs etc. that were tuned for the highest resolution (G750). This is our comparison approach now outlined in the new section "Comparability of experiments". The sub-grid scheme for the grounding line is enabled for the G750 run, therefore we also enable it for the coarser resolutions. For the G750 model, the ISMIP6 protocol do not request a sub-grid scheme for retreat, therefore no sub-grid retreat is enabled for the coarser models. We have rephrased the sentences for clarification.

Furthermore, my understanding with how the text is written, is that the grounding line will most likely not coincide with the calving front for grounded marine termini glaciers.

In most instances the calving front coincide with grounding line. We have now clarified this in the section "Ice flow model ISSM": *"However, at most locations the grounding line coincides with the calving front. Except for the floating tongue glaciers Petermann, Ryder and 79° North, the sub-grid schemes at the grounding line is not applied. The treatment of the calving front evolution depends on the experimental setup and is explained in Sect. 2.3 and 2.4.2."*

The text should be clearer about the description on how the calving front is handled in the model.

In the new version of the manuscript, the sections "2.4 Historical and control experiments" and "2.5.2 Oceanic forcing" now clearly state how the calving front is handled. For the historical, ctrl and ctrl_proj the calving front remains fixed. In the projection experiments the calving front is forced with the retreat masks.

The grid resolution still plays a role even when a sub-grid scale physics is used in a model. This assumption might play a part in the conclusion and, ideally, the authors should run and present a simulation that suggests otherwise.

As our statement about using sub-grid scale physics for the GL but not for the retreat was misleading, we think this comment is obsolete. However, we run a few simulations where we vary the GL treatments which are currently available in ISSM. These experiments reveal that the absolute magnitude of mass loss changes very slightly but the general trend is not altered.

Also, the model uses an unstructured grid and a straightforward convergence analysis similar to when using a uniform grid is more difficult. Please, revise the argumentation in the text (line 228-230).

We added a new section that addresses the "Comparability of the simulations" (see answer to general comment 5 of Reviewer 1). With restructuring the description of the model and the experiment we hope to clarify how the calving front is treated.

6. All the simulations are run with the calving front remaining fixed in space and time besides those with a calving rate mask forcing. This was very confusing as it is not clearly mentioned

in the model assumptions in the appropriate section (it only became clear in the result section). The text should make this really clear in the appropriate section of the paper.

To be clear, the *ctrl*, *ctrl_proj*, the historical and the RCP8.5-Rnone scenarios are run with a fixed calving front. The other projection runs (RCP8.5-Rlow/med/high and OO-Rlow/med) received the retreat parametrization for marine terminating outlet glaciers. We hope with restructuring the appropriate sections this will become clearer now. To keep the atmospheric and oceanic forcing fixed in the control run was a request by the ISMIP6 protocol. In our case the ice sheet mask remains fixed in time and space (i.e. no advance or retreat of the calving front).

For the control experiments we added the following sentence: *"In both control experiments (ctrl and ctrl_proj) the SMB and ice sheet mask remains unchanged to the reference year according to the ISMIP6 protocol."*

For simplicity, we choose the oceanic forcing fixed in the historical scenario. However, we added: *"This is a crude approach but representing the historical mass loss accurately was not a strong priority for our experimental setup."*

I do not understand these different treatments and the text does not discuss it. The paper would benefit from more details behind this reasoning, and, also, more discussion on why their conclusions would hold shall this restriction on Rnone experiments be removed. Right now, Rnone experiments do not benefit from the reduced buttressing and from a stronger signal from bed topography adjustments as the other experiments do. The paper mentions this problem but does not discuss it.

Thanks, that is indeed a very good point that is now better discussed. As now mentioned in the Introduction, we choose the different forcings (retreat activated and not activated) to assess the effect of the oceanic forcing on the different grids separately. We extended the discussion (see lines 416-432).

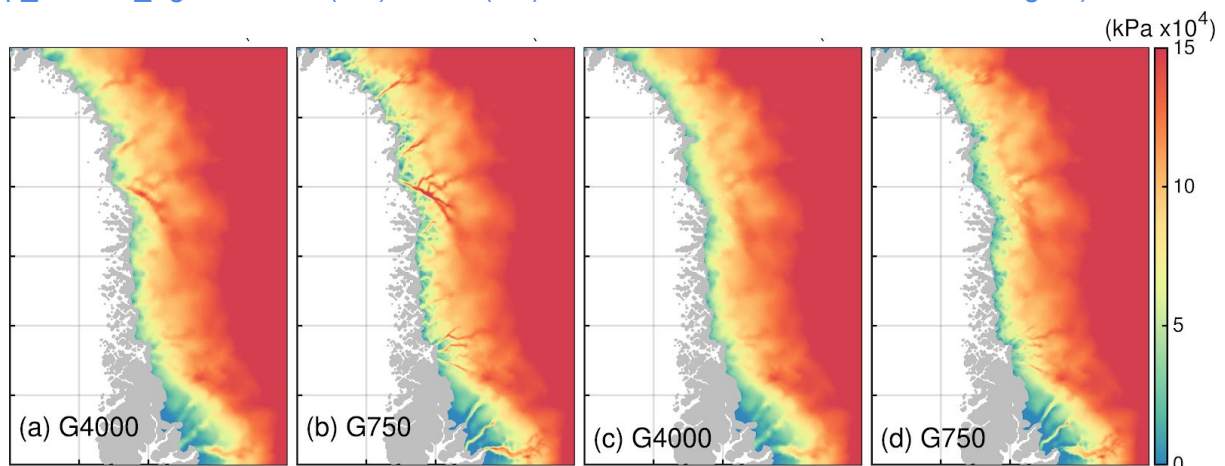
7. The discussion about N , τ_b , τ_d , and the sliding velocity in section 4.4 could be extended more. N decreases with the SMB evolution in these experiments. The SMB perturbations lead to a decrease in ice thickness to which N directly depends on, hence a reduction in τ_b . Also, at higher resolution, the marine portion of the glacier shows deeper bed (figure 10) which will result in a lower N , a lower basal friction and an increase in sliding velocity in order to balance the driving stress. Gagliardini et al. 2007, and Leguy et al. 2014 study these relationships and they can be used as references for the discussions. Also, this discussion item should be tied in with the discussion of the importance of the bed resolution especially when using effective pressure dependent basal friction laws. Oddly enough, these points are being mentioned in the conclusion but not before, why?

We would like to refrain from deepening the analysis to the balance of stresses, as it requires further an analysis of e.g. longitudinal and lateral drag changes as the driving stress is not fully balanced by basal drag in fast flowing areas. Although such an analysis is very important to gain further understanding of the underlying processes it is beyond the scope of this study. Our intention with presenting τ_b and τ_d was to illustrate ongoing changes over the course of the experiments. In doing so, these insights help to understand the driving causes and mechanisms between the employed grids. However, we reorganized the discussion (e.g. the points from the conclusion have now made it into the discussion) and we add new material (Figs. 3, 12 and 13 in the new version of the manuscript) to support our

conclusions. The rephrased section are found in lines 392-407 in the new version of the manuscript. Additionally we add a brief discussion about the friction law used (lines 461-468).

Unfortunately, we placed a slightly wrong statement in the conclusion (“*In general, a reduction of N is overcompensated by a reduction in τ_b , leading to an increase in sliding speed*”, Line 452/453). We detected a non-trivially response: in RCP8.5-Rnone most of the outlet glaciers experience a slow-down along with a decrease in τ_b . For scenarios with considered retreat, we observe a widespread glacier acceleration along with a increase auf τ_b . The latter means, in the coevolving fields N and v_b , the increase of v_b overcompensates the decrease of N (such a behaviour would probably not apparent using a bounded friction law). Please note, that we have adjusted the colormap showing the changes in τ_d and τ_b (Figs. S20 and S21). Reddish (+) shows now an increase and blueish decrease (-).

The connection between N and the bed is not as simple as outlined in your comment. Of course the marine portions in the fine resolution are much deeper as in the coarser resolution. But the ice thickness is also better resolved at higher resolution. Therefore, the deeper troughs/fjords alone do not directly cause a lower N (see figures below showing $p_{ice} = \rho_i * g * thickness$ (a,b) and N (c,d) for G4000 and G750 in a selected region).



Specific comments:

Page 1: Line 16: remove the character “N”.

Done

Line 14-16: “A major response ... ” By invoking the sliding mechanism using effective pressure you are inherently talking about the dependency with respect to the basal sliding law used in the model. I would simply live it as that in the abstract as there is no further modeling details given at that point.

We agree and dropped “(despite no climate-induced hydrological feedback is invoked)”

Page 2: line 34: add the citation of Nowicki et al. 2020.

We added this reference.

Line 44: Please rephrase.

Done.

Line 46: replace “affect” by “affects”.

Done

line 54: replace “well” with “will”.

Done.

last paragraph (line 50-54): be careful with the first sentence here as Fig. 1 clearly shows (with ISSM) that a resolution of 0.5 km was necessary to see a drop in SL contribution and no other models (in this figure) submitted results at that resolution. Also, please clarify that the importance of resolving the ice margins in the initMIP simulations is because they are subjected to the strongest SMB anomalies and SMB anomaly transitions compared to the interior of the ice sheet.

We have rewritten the paragraph to:

“Interestingly, the estimated sea-level contributions show a dependence on grid resolution (Fig. 1). ISM versions with multiple grid resolutions demonstrate that coarser grid resolutions tend to produce a slightly larger mass loss. However, this effect is partly due to the methodological approach by considering a SMB anomaly that is based on the present-day observed SMB. Therefore, ISMs with initial areas larger than observed are subject to more and stronger melting and sharper transitions in SMB. Therefore, coarse resolution models not rendering the present-day ice margin perfectly will likely overestimate ablation.”

Page 3: Line 59: please spell out SIA as it is the first time it is employed in the text.

Done. “SIA” does not appear any longer in the text.

Line 70: “however, the SMB ... ” please clarify what it means and why it matters here. Last sentence: Why is this information of importance? Are you trying to make a point that their choice of Stokes approximation is a limiting factor? As stated, I would simply remove it.

As suggested, the sentence is deleted.

Page 4: Line 74: “which is ... (Church et al., 2013)” this comment feels out of place in what you are trying to say here. I would remove it.

Done. Sentence is removed.

Line 77: “The adequate resolution ... ” please add citation(s) to support this claim. Also, as stated it is quite confusing because increasing the resolution is a good thing (up to a certain point) regardless of the Stokes approximation. The resolution dependency is typically greater with sub-grid scale physical mechanism such as grounding line tracking, ... or when needed to better resolve bed topography.

We have rewritten the sentences to:

“High-resolution models, in turn, require a larger amount of computational resources. Additionally, when increasing the resolution, simple approximations to the momentum balance do not provide an accurate solution (Pattyn et al., 2008). This limitation takes place particularly at the ice sheet margin and at outlet glaciers where all terms in the force balance become equally important (e.g. Pattyn and Durand, 2013). Due to the intensive

computational resources needed to solve the full-Stokes equation, higher-order approximations provide a good compromise to balance model accuracy and computational costs on centennial time scales.”

Line 78: “higher-order approximation is providing ... ” please add citation(s) supporting your claim (for similar reason as previous remark).

See answer to Line 77

Line 82: “to this task” please clarify what you mean here.

We replaced “task” with “grid resolution”.

Line 82: “Therefore, the main ... ” I would suggest beginning a new paragraph with this sentence adding directly what will be the major difference compared to what Aschwanden did (which is very similar).

We do not exactly rewrite the lines as suggested but we mentioned now earlier in the Introduction (as a consequence to Aschwanden’s work):

“... A separation of both responses in future projections experiments would shed some light, how these two main contributors from the GrIS to sea-level are affected by the horizontal resolution....”

In response to the reviewers comment we write here: *“... Beside running the full scenarios (i.e. both oceanic and atmospheric forcing considered), we aim to explore the grid resolution dependence on atmospheric and ocean forcing separately. ...”*

Line 85: “Blatter-Pattyn-type” Is it different than BP? If so, how does it differ? Otherwise remove “type”. Please, add a reference to BP here as it is the first time you mention it and you can remove the one on line 99.

Thanks. We changed it accordingly.

Line 87: “For comparison ... ” What is the relevance of this information here.

We dropped the sentence.

Line 90: “A secondary aim ... ” This sentence is confusing here as it sounds like the aim of this paper is to redo the ISMIP6 exercise.

The sentence is dropped. As suggested by Reviewer 1, the main focus is now on the grid-dependence sensitivity.

Line 91: “which could be valuable ... ” not necessary there.

We dropped this sentence.

Line 91: the footnote on the word “audience” This footnote is confusing. Are there any differences between ISSM and AWI-ISSM? If so the text should highlight these differences to improve clarity. For instance, which release of ISSM did AWI branch from? Was there major development(s) made since then and if so add a reference.

AWI-ISSM denotes the AWI application of ISSM and not any model development. We are working with the developer version of the code, no new branch or anything like that. Differences between different applications of the ISSM’s code occur due to several choices,

e.g. ISSM version, initialization technique, choices of boundary conditions, relaxation strategies, grid resolution, employed approximation to Stokes flow, reference SMB, reference year of the initial state etc. (see Tab 3 and Appendix A in Goelzer et al. (2020).) AWI-ISSM has its own choices for all these components. We just wanted to say AWI-ISSM is not equal to any other application of the ISSM model that contributed to ISMIP6. Most likely, differences occur due to model characteristics and not due to the ISSM version used. We add in “code availability” which version of ISSM is used.

However, as we focus now more on the grid-dependency rather than on model description, we dropped to outline differences between the ISSM contributions to ISMIP6.

Line 99: Blatter-Pattyn is a very expensive model to run. Please clarify what you mean by “balancing computational cost”, are you referring in comparison to full Stokes?

It is costly compared to SIA and SSA, but cheap compared to Stokes. We rewrote the sentence here and gave a few more details above. See answer to Line77. The sentence here reads: *“Here, we make use of the BP approximation to obtain a most accurate solution.”*

Line 102: please add citations for the characteristics of the model (Glen’s flow law, temperature dependent rate factor ...).

Done.

Page 5: Line 104: add “,” after “base”.

Done

Line 104: please add a citation for this form of sliding law. Also, please clarify your choice of sliding law. This formulation is typically avoided as it can grow unboundedly (schoof 2005). Also, it would be good to provide a map of the k^2 friction coefficient.

Thanks, that’s a good point. The choice of the sliding law is based on a long history started a few years ago. We are aware of this limitation and aim to switch to another type of sliding law in the future that considers Iken’s bound. We add a map of the obtained friction coefficient k^2 in the supplement (Fig. S3). The section here is rewritten (see lines 100-109 of the new version of the manuscript) by including a reference for the friction law and give a motivation for the choice of this law.

Line 109: “At lateral ... ” The sentence is confusing, please reword.

Done.

Line 111: Please provide a citation or link for EPSG:3413 grid.

Done. We dropped “EPSG:3413 grid” as we think this is unnecessary information.

Line 122: Please indicate if the grid is fixed throughout the simulation or evolving.

We added *“... which remains fixed in time”*.

Line 124-125: typically, modelers think of high resolution being the smallest mesh size used in a model and the coarse (low) resolution being the biggest one. It is less confusing for RESmin to be the coarsest resolution and RESmax to be the highest.

Yes, that might be true. But we aimed to follow the same conventions given in Goelzer et al. (2018, Tab. 3) and Goelzer et al. (2020, Tab. 4). As a compromise, we changed RESmin to REShigh and RESmax to RESlow.

Line 127: “Additionally, we ... ” This information is out of place here and should be omitted.
Done. Sentences are dropped.

Page 6: Line 136: The sentence here contradicts the title of section 3. Maybe rename section 3 as “Forcing experiments” or something similar, and simply state that you are following the ISMIP6 experimental design.

You are right. We renamed it to “Future forcing experiments”.

Line 138: I suggest writing “Slater et al. (2019a, b)” similarly to what you did on page 9 line 222.

Done.

Line 139-142: Why is it necessary to mention initMIP here?

We have completely shortened the paragraph here and initMIP does not occur anymore.

Page 7: Line 152: there is also a projection control experiment that starts at the end of the historical run. Have you run it?

Yes, we have run the projection control experiment. See answer to general comment 1.

Line 155: “The ensemble ... ” I believe it refers to the ensemble from ISMIP6? If so this sentence does not add any value to the paragraph.

The sentence does not occur any longer. A reference to the ISMIP6 ensemble is only given in the Introduction.

Line 159: Please briefly recall how low, median, and high oceanic forcing were defined.

This is explained later in the text. We added a reference to the section below.

Paragraph 3: “Conducted projection ... ” This paragraph is out of place and should be combined somehow with section 3.3.2. The definitions of the runs (which are highlighted in Table2) could be given at the beginning of the result section.

We have restructured the text to better group the information.

Page 8: Line 191: “That means ... ” This sentence is confusing. Do you mean that grounded and floating ice cells are not allowed to retreat? If so it restricts the purpose of the historical run. Please clarify.

No, grounded and floating points within the ice extent are allowed to advance and retreat. Here we say that the ice front is fixed. And yes, the historical scenario is restricted in its purpose because we are omitting the response of the outlet glacier due to a changing calving front (which is known as a major driver e.g. for causing a rapid increase of ice discharge (Bondzio et al., 2017)). However, we put not too much effort into reproducing the historical mass loss accurately as this is beyond the scope of this paper. We have rephrased the paragraph (see lines 180-185 in the new version of the manuscript).

In the description of the “Ice flow model ISSM” we mentioned: *“However, at most locations the grounding line coincides with the calving front. Except for the floating tongue glaciers Petermann, Ryder and 79° North, the sub-grid schemes at the grounding line will not apply. The treatment of the calving front evolution depends on the experimental setup and is explained in Sect. 2.3 and 2.4.2.”*

Page 9: Line 224: “The imposed ... ” Is this sentence supposed to explain how the prescribed calving front retreat was obtained? If so, say so.

We intended to say that the prescribed calving front retreat must be interpreted as a superposition of several mechanisms. We have rewritten the lines to: *“When employing this parameterization the calving front, retreat and advance of marine-terminating outlet glaciers is directly prescribed as a yearly series of ice front positions. (i.e., is not a result of ice velocity at calving front, calving rate and frontal melt that is used to simulate the calving front position).”*

Page 10: Line 228: “This enables ... ” See the general comments. Additionally, this statement is ambiguous because you are using an unstructured grid. While you can compare the results from the simulation using different grids, you cannot claim your comparison to be consistent to grid resolution. Please rephrase.

You, are right this claim is misleading. We have rephrased the sentence (see “Comparability of experiments”, Lines 232-244 in the new version of the manuscript).

Line 237: The title of section 4.1 reads “Initial state”. This title is confusing. Typically, the initial state is the one obtained at the end of the inversion procedure and the one used as initial condition for the historical and control runs. Please rephrase.

You are right. We renamed the section to *“Historical scenario”*.

Section 4.1: this section contains information that should be stated in section 3.1 such as the restriction of the calving front during the inversion procedure ...

Done. We moved the last sentence from section 4.1 to section 3.1.

Page 11: Line 261: “Similar as ... ” There is no need to repeat this sentence here since the MSD metric is used again.

We dropped the sentence.

Line 268: “As the ice ... ” Please discuss further the reason of keeping the calving front fixed throughout the historical run.

See answer to general comment 6 above.

Line 274: “with the control” The projection runs should be corrected with a projection control run instead which is not discussed in this paper.

See answer to general comment 1 above.

Line 275: “in the absence of additional forcing” This defines the control run. It is an unnecessary repetition.

Done.

Line 276: “ ... as a prediction of actual behavior ... ” This is out of place because the text is talking about the control and have not induced any forcing yet. Please rephrase.

Indeed, we are talking about the control and we aim to stress that the response should not be erroneously interpreted as ongoing/observed mass-loss trends. We aim to explain here how the model drift must be interpreted.

Page 12: Line 279: replace “simulation” with “simulations”.

Done.

Line 282: replace “with” with “to”.

Done.

Line 282: “(see above)” Please refer to a section for clarity (unless you are referring to the mass gain numbers?).

Done.

Page 14: Line 304: replace “compared the total” with “compared to the total”.

Done.

Line 307: remove the repetition of “the”.

Done.

Line 311: replace “RCP8.5-Rnone” with “RCP8.5-Rnone and RCP8.5-Rlow”?

Done. Rewritten to: “*The finer resolutions tend to produce more mass loss in 2100 for the RCP8.5-Rmed/high and OO-Rmed/high experiments. An inverse behaviour is determined for the RP8.5-Rnone experiment. The trend in the RCP8.5-Rlow experiment is not clear.*”

Line 316: replace “lesser than” with “less than”.

Done.

Page 15: Line 347: reword “early in the century an increase” with “an increase early in the century”.

Done.

Page 16: Line 357: replace “worth to mention” with “worth mentioning”.

Done.

Line 359: “remains fixed in time ... ” See my general comment.

[See answer to general comment.](#)

Line 366: replace “reduce” with “reduces,”.

Done.

Line 367: replace “not obvious” with “non obvious”.

Done.

Line 368: remove “come into play”.

Done.

Line 369: “The general picture ... ” Please rephrase.

Done. The sentence now reads: *“The responses of most of the outlet glacier reveal the deduced grid-dependent behaviour where higher resolutions cause an enhanced discharge.”*

Page 17: Line 378: “To study ... grid size” Please rephrase.

We have the sentence slightly rewritten to: “In order to investigate whether the response behaviour is an effect by purely reducing the grid size, we repeated the OO-Rhigh and RCP8.5-Rhigh experiments with a G1000 simulation using re-gridded bed topography and friction coefficient from the G4000 initial state (simulations are not shown).”

Line 392: replace “together an increase” with “together causing an increase”?

Done.

Line 392: replace “thinning an acceleration” with “thinning and acceleration”?

Done.

Line 392: “The transient ... ” Please rephrase the end of this sentence.

Done. Sentence is rewritten to: *“The transient evolution reveals further that thinning and acceleration propagate faster and farther upstream in the finer resolution.”*

Page 18: Line 400: replace “nasal” with “basal”.

Done.

Line 405: add “we” before “find”.

Done.

Line 416: please rephrase end of sentence.

Done.

Line 423: replace “it is worth to investigate this influence isolated” with “it will be worth investigating this influence only”?

Done.

Page 19: Line 428: replace “in numerous cases” with “, in numerous cases,”?

Done

Line 431: replace “assessing the importance of it” with “assessing its importance”?

Done.

Line 434: remove “thus”?

Done.

Tables:

Table 1: Is the computational time listed here for all the experiments or simply for the 86-year run after the historical run?

The table caption states that the computational times are based on a projection run. Following the experiment abbreviations introduced in the overview (Page 7, Line 152), the time span of projection should be clear -> 86-years.

Figures: In the relevant figures, please add a black contour for the grounding line.

In Figs 4 and 6 we add a contour for the grounding line. Depending on the used colormap, the color of the contour in each figure changes. In Fig 10 drawing more lines would be confusing. Also, the grounding line should be identified from geometry alone.

Figure 2: replace "G8000" with "G4000".

Done.

The small ice cap above 79N should not be present for consistency with the text and the other figures in the paper.

Done. The updated figures now present grid resolution only within the initial ice margin.

Figure 5: it should really be Figure 6 since its reference appear after figure 6 in the text.

Thanks, we changed the labels.

Figure 6: it should be relabeled Figure 5 (see figure 5 comment above).

Thanks, we changed the labels.

Figure 9: the subfigure labels b and c are misplaced. What are the units for Year? (I have never seen CE before as a unit).

Subfigure labels are correct. We adopted the figure caption for clarification, given that it caused some confusion.

CE stands for Common Era (https://en.wikipedia.org/wiki/Common_Era) and it is widely used.

Figure 10: the x-axis is labeled "distance". What is it relative to? Please add this reference to the figure.

The distance is a measure of the length along a flow line. We were thinking about to label it as "distance to initial ice front position", but that will not work, because of the different extents of each grid resolution. So, we could set zero distance somewhere, but this would still be an arbitrary point. So we suggest leaving it as is. The distance just helps to identify the correct dimension. We clarified in the caption, that the distance is relative to an arbitrary point.

Also, please try to increase the font size of the labels as they are difficult to read on printed paper.

Done.

Sensitivity of Greenland ice sheet projections to spatial resolution in higher-order simulations: the AWI contribution to ISMIP6-Greenland using ISSM

Martin Rückamp¹, Heiko Goelzer^{2,3}, and Angelika Humbert^{1,4}

¹Alfred-Wegener-Institut Helmholtz-Zentrum für Polar- und Meeresforschung, Bremerhaven, Germany

²Utrecht University, Institute for Marine and Atmospheric Research (IMAU), Utrecht, the Netherlands

³Laboratoire de Glaciologie, Université Libre de Bruxelles, Brussels, Belgium

⁴University of Bremen, Bremen, Germany

Correspondence: Martin Rückamp (martin.rueckamp@awi.de)

Abstract. Projections of the contribution of the Greenland ice sheet to future sea-level rise include uncertainties primarily due to the imposed climate forcing and the initial state of the ice sheet model. Several state-of-the-art ice flow models are currently being employed on various grid resolutions to estimate future mass changes in the framework of the Ice Sheet Model Intercomparison Project for CMIP6 (ISMIP6). Here we investigate the sensitivity to grid resolution on centennial sea-level contributions from the Greenland ice sheet and study the mechanism at play. To this end, we employ the finite-element higher-order ice flow model ISSM and conduct experiments with four different horizontal resolutions, namely 4, 2, 1 and 0.75 km. We run the simulation based on the ISMIP6 core GCM MIROC5 under the high emission scenario RCP8.5 and consider both atmospheric and oceanic forcing in full and separate scenarios. Under the full scenarios, finer simulations unveil up to ~5% more sea-level rise compared to the coarser resolution. The sensitivity depends on the magnitude of outlet glacier retreat, which is implemented as a series of retreat masks following the ISMIP6 protocol. Without imposed retreat under atmosphere-only forcing, the resolution dependency exhibits an opposite behaviour with about ~5% more sea-level contribution in the coarser resolution. The sea-level contribution ~~indicate~~ indicates a converging behaviour ~~≤ 1 km~~ ≤ 1 km horizontal resolution. A driving mechanism for differences is the ability to resolve the ~~bed~~ bedrock topography, which highly controls ice discharge to the ocean. Additionally, thinning and acceleration emerge to propagate further inland in high resolution for many glaciers. A major response mechanism is sliding (~~despite no climate-induced hydrological feedback is invoked~~), with an enhanced feedback on the effective normal pressure ~~N~~ at higher resolution leading to a larger increase in sliding speeds under scenarios with outlet glacier retreat.

Copyright statement. TEXT

1 Introduction

20 Climate change is the major driver of global sea-level rise (SLR), which has been shown to accelerate (Nerem et al., 2018; Shepherd et al., 2019). The Greenland ice sheet (GrIS) has contributed about 20% to sea-level rise during the last decade (Rietbroek et al., 2016). Holding in total an ice mass of ~ 7.42 m sea-level equivalent (SLE) (Morlighem et al., 2017), its future contribution poses a major societal challenge. Since 1992, the GrIS mass loss is controlled on average at 52% by surface mass balance (SMB), with the remainder of 48% being due to increased ice discharge of outlet glaciers into the surrounding ocean
25 (Shepherd et al., 2019).

While the relative importance of outlet glacier discharge for total GrIS mass loss has decreased since 2001 (Enderlin et al., 2014; Mouginot et al., 2019) and is expected to decrease further in the future (e.g. Aschwanden et al., 2019), it remains an important aspect for projecting future sea-level contributions from the ice sheet on the centennial timescale. (Goelzer et al., 2013; Fürst et al., 2015). A (non-linear) dynamic response of the ice sheet is caused by changes in the atmospheric and
30 oceanic forcing, that may trigger glacier acceleration and thinning of outlet glaciers. Moreover, processes such as SMB and ice discharge are mutually competitive in removing mass from the ice sheet (Goelzer et al., 2013; Fürst et al., 2015). Beside this interplay, a simple extrapolation of observed GrIS mass loss trends over the next century is not justified, as high temporal variations in SMB and glacier acceleration are apparent (e.g. Moon et al., 2012). Therefore, reliable ice sheet models (ISMs) forced with future climate data must be driven for policy relevant sea-level projections on century time scales.

35 The Ice Sheet Model Intercomparison Project (~~ISMIP6, Nowicki et al., 2016~~) ([ISMIP6, Nowicki et al., 2016, 2020b](#)) is an international community effort striving to improve sea-level projections from the Greenland and Antarctic ice sheets. Based on previous efforts like SeaRISE (Bindschadler et al., 2013; Nowicki et al., 2013) and ice2sea (e.g., Gillet-Chaulet et al., 2012), ISMIP6 continues to fully explore the sea-level rise contribution and associated uncertainties. The effort is aligned with the Coupled Model Intercomparison Project Phase 6 (CMIP6, Eyring et al., 2016) to provide input for the upcoming assessment report
40 of the Intergovernmental Panel on Climate Change (IPCC AR6). [The general strategy is to use outputs from CMIP5 and CMIP6 climate models to derive atmosphere and ocean fields for forcing ISMs. Goelzer et al. \(2020\) and Nowicki et al. \(2020a\) analyse the future sea-level contribution from multi-model ensembles for ISMIP6-projection-Greenland. The major aim of Goelzer et al. \(2020\) is to provide future sea-level change projections and related uncertainty in a consistent framework.](#)

Despite substantial progress in ice sheet modelling in the last decades and years, a challenging goal remains to narrow uncer-
45 tainties and improve [the](#) reliability of future sea-level projections from the two big ice sheets. Up to date, it is recognized that the largest uncertainty sources are related to the initialization of the ISM or stem from the external forcing (~~Goelzer et al., 2020~~)

~~The first ISMIP6 project initMIP-Greenland (Goelzer et al., 2018) particularly targeting (Goelzer et al., 2018, 2020). Goelzer et al. (2018) compared~~ the initialization techniques used ~~in the by different~~ ice sheet modelling ~~community groups~~. The schematic forward
50 experiment was not designed to estimate realistic sea-level contribution, but it provides valuable insights how the initial state of an ISM ~~affect~~ [affects](#) the ice sheet response. Under a predefined SMB anomaly, mass losses reveal a large spread. Although

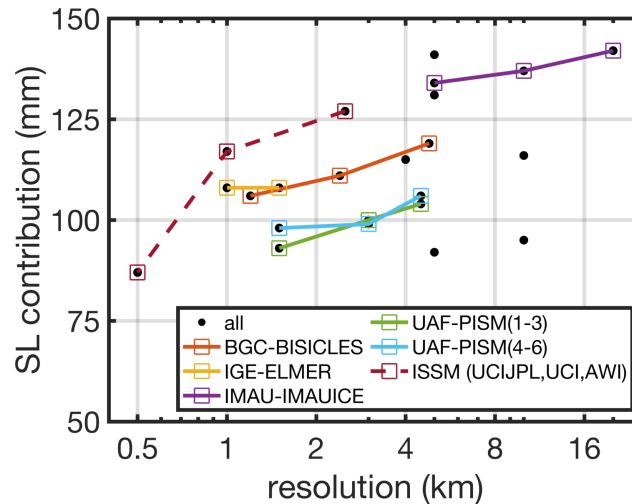


Figure 1. Results from the initMIP-Greenland exercise (Goelzer et al., 2018). Sea-level contribution versus (minimum) horizontal grid resolution of each participating ISM. Equal model versions but different grid resolutions are connected with a coloured line. ISSM model versions are connected with a coloured dashed line. Note the logarithmic scale of the x-axis. [For unstructured meshes the finest resolution is displayed.](#)

the spread is attributed to the [large broad](#) diversity in model approaches, initMIP-Greenland shows notable improvements (e.g., a reduced model drift) and more consistent results compared to earlier large scale intercomparison exercises.

~~The results of the initMIP exercise are certainly affected by other not obvious factors than the initialization.~~ Interestingly, the estimated sea-level contributions show [barely](#) a dependence on grid resolution (Fig. 1). ISM versions with multiple grid resolutions demonstrate that coarser grid resolutions tend to produce a slightly larger mass loss. This effect is partly due to the methodological approach by considering a SMB anomaly that is based on the present-day observed SMB. [That means ISMs with initial areas larger than observed are subject to more and stronger melting and sharper transitions in SMB.](#) Therefore, coarse resolution models not rendering the present-day ice margin perfectly [well will](#) likely overestimate ablation.

~~Greve and Herzfeld (2013) explored how spatial grid resolutions of 20, 10, and 5 km impact the ice mass change under standardized future climate scenarios. The simulations demonstrated that the absolute ice volumes in the initial state depend significantly on the resolution; the 5 km resolution setup holds a SLE that is approx. 0.1 m lower than the 20 km resolution setup. However, the sensitivities in the forward experiments vary only by a few percents and do not show a consistent trend among all conducted experiments. A limitation of this study is the employed SIA approximation, which is known to be invalid for fast-flowing outlet glaciers, and the medium to coarse resolution range which is insufficient to resolve the narrow and confined outlet glaciers in Greenland correctly.~~

~~Aschwanden et al. (2016) highlighted the importance of grid resolution on GrIS flow behaviour by accurately resolving the ice geometry. Their result indicates, that a resolution of < 1 km is required to replicate the overall flow pattern without spatially tuning relevant parameters. In a subsequent study, Aschwanden et al. (2019) performed large-scale GrIS projections~~

70 on-millennial time scales under RCP 2.6, 4.5 and 8.5 scenarios. Besides their ensemble predictions, they present individual
grid-dependent simulations (ranging from 0.6 to 18 km) (simulations G600-G18000 in Tab. 1 in Aschwanden et al., 2019). There
is no clear trend in the ~~However, increasing the spatial resolution comes along with the ability to resolve the geometry and
to track outlet glacier behaviour (Greve and Herzfeld, 2013; Aschwanden et al., 2016). Some previous works focused on the
dependence of future mass loss of the GrIS on grid resolution (Greve and Herzfeld, 2013; Aschwanden et al., 2019). In these~~
75 ~~studies no clear conclusion how the resolution affects the mass loss was found. This was partly explained by the competing
tendencies of SMB and ice discharge that are differently resolved by the adopted resolutions. A separation of both responses
in future projections experiments would elucidate how these two main sea-level contribution as a function of grid resolution
identifiable. The simulation with a grid spacing of 1800 m tends to produce the largest sea-level contribution compared to the
other resolutions. Ice discharge (consists in Aschwanden et al. (2019) as the sum of mechanical calving and frontal melt) for
80 grid resolutions 1800 m and smaller are very similar and likely will not change significantly under further grid refinement;
however, the SMB still lowers when the resolution increases (pers. comm. A. Aschwanden). Their study is based on shallow
ice approximation, including shallow shelf approximation for sliding.~~

Increasing the spatial resolution comes along with the ability to resolve the geometry and to track outlet glacier behavior
which is a prerequisite formulated by the IPCC (Church et al., 2013) to improve projections. In turn, it requires ~~contributors~~
85 ~~from the GrIS are affected by the horizontal resolution. Most likely coarse grids underestimate ice discharge as ice flow patterns
and cross-sections of outlet glacier geometries are not well captured (Greve and Herzfeld, 2013; Aschwanden et al., 2016).
High-resolution models, in turn, require a larger amount of computational resources. To identify an acceptable limit in spatial
resolution~~ Unfortunately, when increasing the resolution, simple approximations to the momentum balance do not provide an
accurate solution (Pattyn et al., 2008). This limitation takes place particularly at the ice sheet margin and at outlet glaciers where
90 all terms in the force balance become equally important (e.g. Pattyn and Durand, 2013). Due to the intensive computational
resources needed to solve the full-Stokes equation, higher-order approximations provide a good compromise to balance model
accuracy and computational costs on centennial time scales.

Determining whether increased model resolution is worth the extra computation time would be valuable to ~~balance computational
amount, data storage and particularly to~~ make progress in narrowing uncertainties in ice sheet projections, even if only by a
95 few percent. ~~The adequate resolution is also depending on the approximation of the momentum balance. For capturing the
dynamics of outlet glaciers, higher-order approximation is providing a suitable physical basis and is therefore chosen for this
study.~~

~~The current per cent. The ISMIP6-projection-Greenland multi-ensemble effort analyse the future sea-level contribution from
various ISMs (Goelzer et al., 2020). Though the exercise shows that models with low and high resolution are found at the upper
100 and lower bound of sea-level contribution, though no specific analysis to this task the grid resolution is performed. Therefore,
the~~

The main intention of this paper is to ~~evaluate the complement the study by Goelzer et al. (2020) by evaluating the~~ sensitivity
of the simulated GrIS response to global warming due to different horizontal grid resolutions by one single ISM.

To this end, the Ice Sheet System Model (ISSM, ~~?~~) is applied to the GrIS with the higher-order Blatter-Pattyn-type approximation and Beside running the full scenarios (i.e. both oceanic and atmospheric forcing considered), we aim to explore the grid resolution dependence on atmospheric and ocean forcing separately. Therefore, the full scenarios are complement with experiments where either a changing SMB or the interaction of the glacier with the ocean is omitted. The simulations of the GrIS are performed with the Ice Sheet System Model (ISSM, Larour et al., 2012) and adopted spatial resolutions ranging from medium to high (4 and 0.75 km at ~~fast-flowing-fast-flowing~~ outlet glaciers, respectively). For comparison, the resolutions covered by the ISMs in the ISMIP6-projection-Greenland-exercise ranges between 0.25 km (JPL-ISSM) and 16 km (IMAU-IMAUICE1). Simulations are forced by climate-The future scenarios build on climate forcing data from the CMIP5 global circulation model (GCM) MIROC5 under the Representative Concentration Pathway (RCP, Moss et al., 2010) 8.5 following the ISMIP6 protocol (Nowicki et al., 2020b). A secondary aim of this paper is to describe in detail how the ISMIP6 exercise has been conducted using ISSM, which could be valuable for a broader audience¹.

2 Ice flow model ISSM

2 Methods and experiments

Before presenting the concept of this study, we aim to address the terminology used for clarity. Following the glossary in Cogley et al. (2011), ice discharge is computed as the product of ice thickness h and the depth-averaged velocity \bar{v} . In the following, the lower-case q ($\text{Gt a}^{-1} \text{m}^2$) refers to the local ice discharge at a point, and the upper-case Q (Gt a^{-1}) refers to the glacier-wide quantity (analogous for other quantities such as glacier-wide calving D and local calving d). Quantities at the margin are reckoned in the normal direction.

2.1 Ice flow model ISSM

The model applied here is the Ice Sheet System Model (~~ISSM, ?~~)(ISSM, Larour et al., 2012). It has been applied successfully to the GrIS in the past (Seroussi et al., 2013; Goelzer et al., 2018; Rückamp et al., 2018, 2019a) and is also used for studies of individual drainage basins of Greenland, e.g. the North East Greenland Ice Stream (Choi et al., 2017), Jakobshavn Isbræ (Bondzio et al., 2017) and Petermann Glacier (Rückamp et al., 2019b).

ISSM is designed to use variable ice flow approximations ranging from shallow ice approximation to full-Stokes and has also the capability to perform inverse modelling to constrain unknown parameters.

Here, we make use of the ~~Blatter-Pattyn higher-order approximation (BP, Blatter, 1995; Pattyn, 2003) to balance model accuracy and computational costs~~BP approximation to obtain a most accurate solution even though computational time increased compared to simpler models (e.g. Aschwanden et al., 2019). The system of equations are solved numerically with the finite element method on an unstructured grid. The latter allows for variable resolution in key areas of the ice sheet, e.g. marine terminating outlet glaciers. State and state variables are computed on each vertex of the mesh using piecewise-linear finite

¹ Although there are various ISSM contributions from different groups with different model characteristics to ISMIP6-projection-Greenland, we will simply use 'ISSM' for the ISMIP6 contribution AWI-ISSM in the following text. At some instances we will use AWI-ISSM to avoid any misunderstanding.

elements. The ice rheology is treated with a regularized Glen flow law (Glen, 1955), a temperature-dependent rate factor for cold ice, and a ~~water-content-dependent~~ watercontent-dependent rate factor for temperate ice (Lliboutry and Duval, 1985).

At the ice base, sliding is allowed everywhere and the basal drag τ_b ~~is written as follows~~ is written as follows a linear viscous law (Weertman, 1957; Budd et

$$\tau_{b,i} = -k^2 N v_{b,i}, \quad (1)$$

where $v_{b,i}$ is the basal velocity vector in the horizontal plane and $i = x, y$. Although this type of friction law is often used in ice sheet modelling (Morlighem et al., 2010; Price et al., 2011; Gillet-Chaulet et al., 2012; Seroussi et al., 2013), it implies that the basal drag can increase without a bound. It was shown, that inducing an upper ratio of τ_b/N (Iken's bound) is more justified (Iken, 1981; Schoof, 2005; Gagliardini et al., 2007; Leguy et al., 2014; Joughin et al., 2019). However, we choose this type of friction law as it is commonly used in ISMs making use of inverse methods to constrain the basal friction (Morlighem et al., 2010; Larour et

The friction coefficient k^2 is assumed to cover bed properties such as bed roughness. ~~Here, k^2 is retrieved by an inversion technique (see sect. 2.2).~~ The effective pressure is defined as $N = \rho_i g h + \min(0, \rho_w g z_b)$, where h is the ice thickness, z_b the glacier base and $\rho_i = 910 \text{ kg m}^{-3}$, $\rho_w = 1028 \text{ kg m}^{-3}$ ~~$\rho_i = 910 \text{ kg m}^{-3}$, $\rho_w = 1028 \text{ kg m}^{-3}$~~ the densities for ice and sea water, respectively. At lateral boundaries ~~The parametrization accounts for full water-pressure support from the ocean wherever the ice sheet base is below sea-level, even far into its interior where such a drainage system may not exist. At marine-terminating glaciers~~ water pressure is applied ~~at marine-terminating glaciers~~ and zero pressure along ~~land-terminating~~ land-terminating ice cliffs. A traction-free boundary condition is imposed at the ice/air interface.

The ISSM model domain for the Greenland ice sheet covers the present-day main ice sheet extent ~~on the EPSG:3413 grid~~, and includes the current floating ice tongues (e.g., Petermann, Ryder and 79° North glaciers). The geometric input is Bed-Machine v3 (Morlighem et al., 2017). Thickness, bedrock and ice sheet mask is clipped to exclude glaciers and ice caps surrounding the ~~ice sheet proper~~ main ice sheet. The initial ice sheet mask is manually retrieved from the data coverage of the MEASURE velocity ~~dataset (Joughin et al., 2010, 2016)~~ data set (Joughin et al., 2016, 2018) to ensure an available target for the employed basal friction inversion (~~see below~~ sect. 2.2). A minimum ice thickness of 1 m is applied. Grounding line evolution is treated with a sub-grid parameterization scheme, which tracks the grounding line position within the element (Seroussi et al., 2014). A sub-grid parameterization on partially floating elements for basal melt is applied (Seroussi and Morlighem, 2018). The basal melt rate below floating tongues is parameterized with a Beckmann–Goosse relationship (Beckmann and Goosse, 2003). ~~The melt factor is roughly adjusted such that melting rates correspond to literature values (e.g. Wilson et al., 2017; Rückamp et al., 2019b).~~ In this parameterization ocean temperature and salinity are set to -1.7°C and 35 Psu, respectively. The melt factor is roughly adjusted such that melting rates correspond to literature values (e.g. Wilson et al., 2017; Rückamp et al., 2019b). However, at most locations the grounding line coincides with the calving front. Except for the floating tongue glaciers Petermann, Ryder and 79° North, the sub-grid schemes at the grounding line is not applied. The treatment of the calving front evolution depends on the experimental setup and is explained in Sect. 2.3 and 2.4.2.

Table 1. Summary of models and their mesh characteristics. Computational time is based on a projection run under MIROC5 RCP 8.5 and medium ocean forcing.

Model name (this study)	Model name RES_{high} (ISMIP6) (km)	RES_{min} RES_{low} (km)	RES_{max} number of elements	time step Δt (yr)	computational time (minutes)	number of cores
G4000	-4	7.5	1 169 546	0.100	83	90*
G2000	-2	7.5	1 951 586	0.050	252	162*
G1000	AWI-ISSM2-1	7.5	4 241 020	0.025	640	342 [†]
G750	AWI-ISSM3-0.75	7.5	6 220 928	0.010	1731	702 [†]

* Intel Xeon Broadwell CPU E5-2697 v4, 2.3 GHz on the AWI HPC system Cray CS400.

[†] Intel Xeon Broadwell CPU E5-2695 v4, 2.1 GHz on the DKRZ HPC system Mistral.

Model calculations with ISSM are performed on a horizontally unstructured grid which remains fixed in time. To limit the number of elements while maximizing the horizontal resolution in regions where physics demands higher accuracy, the horizontal mesh is generated with a higher resolution of RES_{min} RES_{high} in fast-flowing regions (observed ice velocity $> 200 \text{ m a}^{-1}$) and a coarser resolution of RES_{max} RES_{low} in the interior. This adaptive strategy allows a variable resolution in key areas of the ice sheet, e.g. marine-terminating outlet glaciers. Experiments are carried out at four different horizontal grid resolutions with RES_{min} RES_{high} equal to 4, 2, 1, and 0.75 km (Tab. 1 and Fig. 2). The experiments G1000 and G750 are a contribution to the ISMIP6 ensemble, termed AWI-ISSM2 and AWI-ISSM3 in Goelzer et al. (2020), respectively. Additionally, we contributed with AWI-ISSM1 to ISMIP6, but this model version is neglected here as its has an alternative meshing approach and is therefore not directly comparable.

The distribution of mesh vertices at numerous outlet glaciers is depicted in Figs. S3 to S16. The horizontal resolution of a triangle is defined by its minimum edge length. S6 to S19. In Figure 3, the interpolated bed elevation for two selected regions and grid resolutions is illustrated. Overall, the bedrock topography of the finer resolution shows deeper and fjord-like troughs which is closer to the BedMachine dataset.

Independent of the horizontal resolution, the vertical discretization comprises 15 terrain-following layers, refined towards the base where vertical shearing becomes more important. Please note, that G1000 and G750 correspond to the ISMIP6 contributions AWI-ISSM2 and AWI-ISSM3, respectively, in Goelzer et al. (2020).

During all transient runs, we neglect an evolution of the thermal field. This is justified as it was shown by Seroussi et al. (2013) and Goelzer et al. (2018, see submissions AWI-ISSM1 and 2) that the temperature field and its change has a negligible effect on century time-scale projections of the GrIS.

3 ISMIP6 experimental design

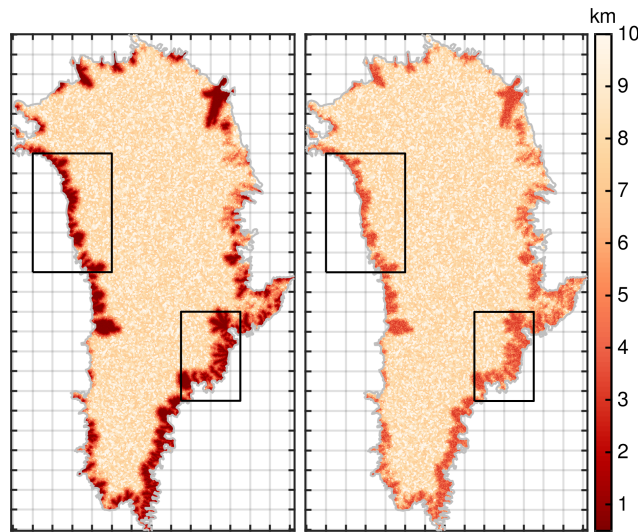


Figure 2. Horizontal mesh resolution (in km) used for G750 (a) and G8000-G4000 (b). Data are clipped at 0.5 and 10 km. The horizontal resolution of a triangle is defined by its minimum edge length. The grey line delineates the initial ice domain from. Grey grid lines indicate 100 km. The black boxes indicate the initialization northwestern and southeast subsets used in following figures.

It is beyond the scope of this paper to present the details of the ISMIP6 protocol and experimental design. Therefore, we aim to briefly outline the external forcing approach. Further details are given in Goelzer et al. (2020), Nowicki et al. (2020a), Fettweis et al. (2020), and Slater et al. (2019).

The experimental design for the

2.1 Overview of experiments

The ISMIP6 projections is based on the precursor initMIP-Greenland (Goelzer et al., 2018), which studied the model initialization techniques used in the ice sheet modelling community. For the ISMIP6-Greenland projections groups were asked to participate with their already existing or improved initMIP setup. As protocol requests the initialization mode prior or to the ISMIP6 philosophy follows the "come as you are" approach each model involved has different flavours in model characteristics and probably in the assigned reference year. Therefore, in a series of experiments, the first ISMIP6 experiment, termed historical, is dedicated to bring each model to the common ISMIP6 start date at end of 2014 from where on projection start date. If the initialization date is before the start of the projections, a short historical run is needed to advance the ISM from the reference date to the end of 2014. From this date, the future climate scenarios branch off. Given the fact that every model initialization has its own evolving response to a prescribed experiment, an unforced Unforced constant-climate control experiment is experiments are defined to capture the model drift with respect to the ISM reference climate -

and the ISMIP6 projection start date. The set of experiments are described in the following sections but can be summarized as follows:

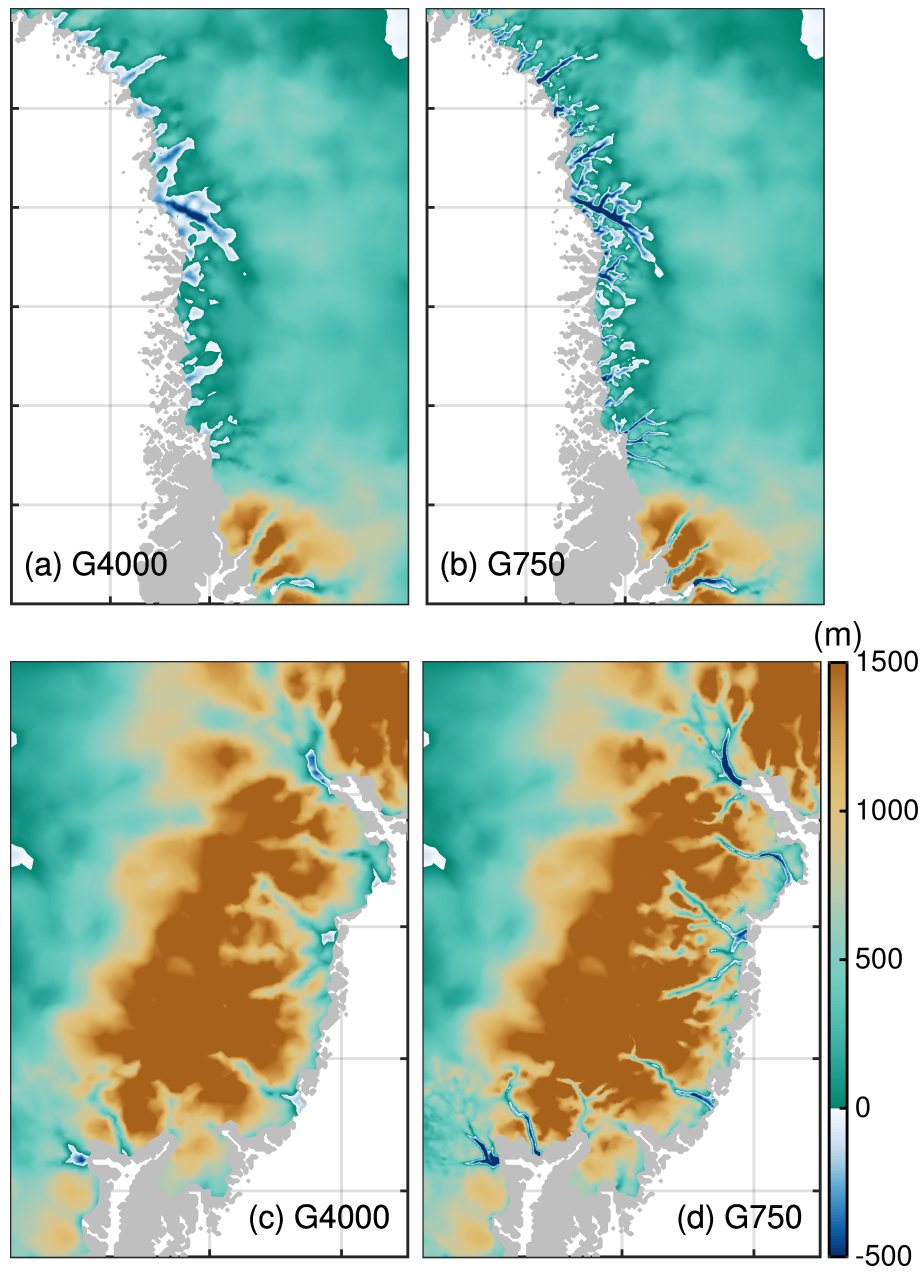


Figure 3. [G4000 and G750 bedrock topography for the northwestern region \(a,b\) , respectively, and for the southeast region \(c,d\), respectively.](#)
[Region subsets are shown in See Fig. 2.](#)

205 – initialization: experiment to retrieve the initial state of the model.

- ~~control~~ctrl: experiment where the climate is held constant to the reference climate (~~lasts until~~ from January 1991 to end of December 2100).
- ctrl_proj: experiment where the climate is held constant to the reference climate (from January 2015 to end of December 2100).
- 210 - historical: experiment to bring model from the initialization state to ISMIP6 projection start date (~~lasts until~~ from January 1991 to end of December 2014).
- projection: future climate scenario (from January 2015 to end of December 2100).

~~We aim to study the effect of grid resolution on ice mass changes. Therefore, we selected the MIROC5 under RCP8.5 climate which is a core experiment in ISMIP6. The GCM MIROC5 was selected as it performs well in the historical period and represents a plausible climate near Greenland (?). The ensemble projections will be explored in separate papers by Goelzer et al. (2020) and Nowicki et al. (2020a).~~

~~Conducted projection experiments and the corresponding experiment labels used in this study are summarized in Tab. 2. In the ISMIP6 ensemble study, the experiments with low, medium, and high oceanic forcing (explained below) are needed to quantify related uncertainties. Here, we run MIROC5 RCP8.5 with low, medium and high oceanic forcing as we expect increasing ice discharge with larger retreat of outlet glaciers. Thus, they can be interpreted as a weighting between the competing tendencies of SMB and ice discharge. If both external forcings are considered the scenarios are termed as 'full' in the following. In addition we perform simulations where only the atmospheric forcing (RCP8.5-Rnone) or only tidewater glacier retreat (OO-Rmed/high) is at play. The RCP8.5-Rnone and OO-Rmed/high experiments are consequently a setup to explore the impact of SMB and ice discharge on mass loss separately.~~

225 Please note, that for the presented study more experiments (e.g., atmospheric only) from extended model versions (larger range of horizontal resolutions) are performed other than available in the ISMIP6-projection-Greenland-exercise.

~~Summary of projection experiments based on MIROC5-RCP8.5 climate data. Experiment label atmospheric forcing oceanic forcing RCP8.5-Rlow-SMB anomaly low RCP8.5-Rmed-SMB anomaly med RCP8.5-Rhigh-SMB anomaly high RCP8.5-Rnone SMB anomaly OO-Rmed--med OO-Rhigh--high~~

230 2.2 Initialization experiment

The initialization state of ISSM is based on data assimilation and inversion for determining the basal friction coefficient. Before the inversion, a relaxation run assuming no sliding and a constant ice temperature of -10°C is performed to avoid spurious noise that arises from errors and biases in the ~~datasets~~data sets. To ensure that the relaxed geometry does not deviate too much from the observed geometry, the relaxation is conducted over one year. However, while inverse modelling is well established

235 for estimating basal properties, the temperature field is difficult to constrain without performing an interglacial thermal spin-up. Therefore, we rely on a temperature field that was obtained by a hybrid approach between paleoclimatic thermal spin-up and basal friction inversion. This method was developed for the AWI contribution in initMIP-Greenland (Goelzer et al., 2018) and

further improved in Rückamp et al. (2018) by using the geothermal flux pattern from Greve (2005, scenario hf-pmod2). Here, we initialize the ice rheology on the four employed G4000–G750 grids by interpolating the 3D temperature and watercontent fields from the hybrid spin-up in Rückamp et al. (2018)~~on the ISSM grid. Equivalent we interpolate the basal melt. The basal melting rates of grounded ice are equivalently interpolated. During all transient runs, we neglect an evolution of the thermal field. This is justified as it was shown by Seroussi et al. (2013) and Goelzer et al. (2018, see submissions AWI-ISSM1 and 2) that the temperature field and its change has a negligible effect on century time-scale projections of the GrIS.~~

The ~~inversion approach infers~~ main ingredient to the initialization is the inversion to infer the basal friction coefficient k^2 in Eq. 1 ~~by minimizing~~. This approach minimizes a cost function that measures the misfit between observed and modelled horizontal velocities (Morlighem et al., 2010). The cost function is composed of two terms which fit the velocities in fast- and slow-moving areas. A third term is a Tikhonov regularization to avoid oscillations. The parameters for weighting the three contributions to the cost function are taken from Seroussi et al. (2013). We leverage horizontal surface velocities from the MEASURE project (~~Joughin et al., 2010, 2016~~)(Joughin et al., 2016, 2018), as the ~~dataset data set~~ dataset data set with almost no gaps over GrIS is suitable for basal friction inversion.

The assigned reference year is 1990. This date is not in agreement with the timestamps of the BedMachine ~~dataset data set~~ (reference time is 2007) and the MEASURE velocity ~~dataset data set~~ (temporal coverage from 2014 to 2018). However, we ignore the contemporaneity requirement in the inversion approach and ~~place more value put more weight~~ on to start the projections at the end of the assumed GrIS steady-state period (e.g. Ettema et al., 2009). All transient simulations start from the initial state, that means, we do not perform a subsequent relaxation run to bring the model to a steady-state (see sect. 2.5).

2.3 ~~Historical scenario To bring our and control experiments~~

In both control experiments (ctrl and ctrl_proj), the SMB and ice sheet mask remains unchanged to the reference year according to the ISMIP6 protocol. To advance the model from the reference time to the projection start date, the historical scenario is needed. During the historical period, yearly cumulative SMB is taken from the RACMO2.3p2 product (Noël et al., 2018) for the years from 1990 to 2015. ~~In this scenario the ice front is fixed in time. That means calving exactly compensates the outflow through the margins, and initially glaciated points are not allowed to become ice-free. For simplicity, the ice sheet extent remains unchanged to the reference year. This is a crude approach but representing the historical mass loss accurately was not a strong priority for our experimental setup. As the ice front is not moving in these three scenarios ice discharge Q equals calving D .~~

265 2.4 ~~Future climate scenarios~~

2.4 Future forcing experiments

It is beyond the scope of this paper to present the details of the ISMIP6 protocol and experimental design. Therefore, we aim to briefly outline the external forcing approach. Further details are given in Goelzer et al. (2020), Nowicki et al. (2020b), Fettweis et al. (2020), and Slater et al. (2019, 2020).

Table 2. Summary of projection experiments based on MIROC5-RCP8.5 climate data.

Experiment label	atmospheric forcing	oceanic forcing	combination
RCP8.5-Rlow	SMB anomaly	low	full
RCP8.5-Rmed	SMB anomaly	med	full
RCP8.5-Rhigh	SMB anomaly	high	full
RCP8.5-Rnone	SMB anomaly	-	atmospheric only
OO-Rmed	-	med	ocean only
OO-Rhigh	-	high	ocean only

270 As we aim to study the effect of grid resolution on ice mass changes, we run the future scenarios based on climate data from one single GCM. The GCM MIROC5 was selected as it performs well in the historical period and represents a plausible climate near Greenland (Barthel et al., 2020). The GCM output is used to separately derive ISM forcing for the interaction with the atmosphere and the ocean. We set up experiments where both external forcings are considered; these scenarios are termed as 'full' in the following (RCP8.5-Rlow/med/high). In addition, we perform simulations where either the atmospheric forcing (RCP8.5-Rnone) or the marine-terminating outlet glacier retreat (OO-Rmed/high) is at play. The conducted projection experiments and the corresponding experiment labels used in this study are summarized in Tab. 2 and are explained in the following sections.

2.4.1 Atmospheric forcing

280 ISMIP6 provide surface forcing [datasets](#) [data sets](#) for the GrIS based on CMIP GCM simulations. The GCM output is dynamically downscaled through the higher-resolution regional climate model (RCM) MAR v3.9 (Fettweis et al., 2017). The latter allows to capture narrow regions at the periphery of the Greenland ice sheet with large SMB gradients, which are likely not captured by the GCMs. The climatic SMB that is used as future climate forcing reads

$$\text{SMB}_{\text{clim}}(x, y, t) = \text{SMB}_{\text{ref}}(x, y) + \Delta\text{SMB}(x, y, t) + \text{SMB}_{\text{dyn}}(x, y, t), \quad (2)$$

with the anomaly defined as

$$285 \Delta\text{SMB}(x, y, t) = \text{SMB}(x, y, t)_{\text{GCM-MAR}} - \overline{\text{SMB}}(x, y)_{\text{GCM-MAR}}^{1960-1989}, \quad (3)$$

where $\text{SMB}(x, y, t)_{\text{GCM-MAR}}$ is the direct output of MAR using the GCM climate data and $\overline{\text{SMB}}(x, y)_{\text{GCM-MAR}}^{1960-1989}$ the corresponding mean value over the reference period (from January 1960 to December 1989). As the reference SMB field $\text{SMB}_{\text{ref}}(x, y)$, we choose the downscaled RACMO2.3p2 product (Noël et al., 2018) whereby a model output was averaged for the period 1960–1990. This period is chosen as the ice sheet is assumed close to steady-state in this period. (e.g. Ettema et al., 2009). The SMB deduced by MAR is processed on a fixed topography (off-line), consequently local climate feedback processes due to the evolving surface in the projection experiments are not captured. The SMB height-elevation feedback is

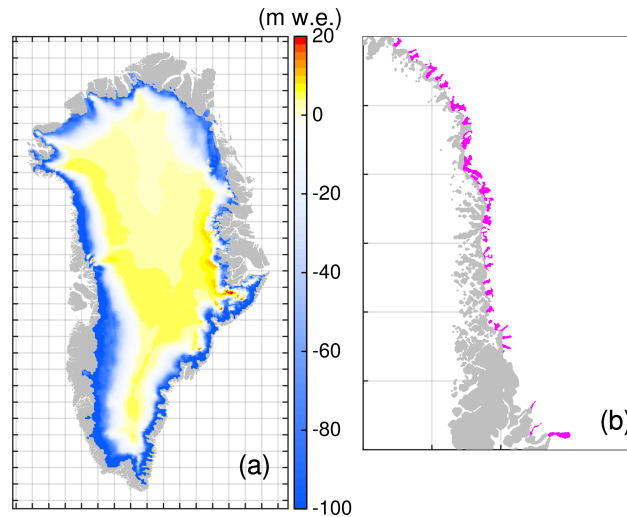


Figure 4. Atmospheric and oceanic forcing. (a) Spatial pattern of the cumulative (2015–2100) SMB anomaly based on MIROC5-RCP8.5 and downscaled with MAR (Fettweis et al., 2020). (b) Retreat of tidewater-marine-terminating outlet glaciers in the northwestern region under RCP8.5-Rhigh scenario. Purple areas indicate retreated areas in 2100. Region subsets are shown in See Fig. 2.

considered with a dynamic correction SMB_{dyn} to the SMB_{clim} following Franco et al. (2012)

$$SMB_{dyn}(x, y, t) = dSMBdz(x, y, t) \times (z_s(x, y, t) - z_{ref}(x, y)). \quad (4)$$

The surface elevation changes are taken from the ISM elevation $z_s(x, y, t)$ while running the simulation and the corresponding
 295 ISM reference elevation $z_{ref}(x, y)$ from the initialization state. The yearly patterns of $\Delta SMB(x, y, t)$ and $dSMBdz(x, y, t)$ are
 provided by ISMIP6. A cumulative SMB anomaly over the projection period is shown in Fig. 4a.

2.4.2 Oceanic forcing

~~Different strategies for oceanic forcing are part of the ISMIP6 protocol. Here,~~ For the oceanic forcing we rely on the
 standard approach which is an empirically-derived, sector-averaged calving front retreat as a function of climate forcing. In this
 300 approach, the oceanic forcing is translated into an outlet glacier retreat parametrization (~~?Slater et al., 2019~~). It parameterizes
~~calving frontretreat as a function of~~ empirically derived outlet glacier parametrization retreat by Slater et al. (2019, 2020). This
 method circumvents the problem of employing a physically-based calving law and frontal melting rates based on GCM output.
When employing this parameterization the calving front, retreat and advance of marine-terminating outlet glaciers is directly
prescribed as a yearly series of ice front positions. (i.e., is not a result of ice velocity at calving front, calving rate and frontal
 305 melt that is used to simulate the calving front position). Here, the binary retreat masks (i.e., ice and non-ice covered cells) are
interpolated to the native grid by nearest neighbour interpolation. Retreat occurs once a cell is fully emptied.

Though this parameterization is a strong simplification, it builds on projected submarine melting (taking into account changes
 in ocean temperature and surface meltwater runoff from a GCM). The parametrization is not applied to the individual glaciers

but over a predefined geographical region. Based on the numerous retreat trajectories, a medium retreat scenario as the trajectory with the median retreat at 2100 is defined. To cover uncertainty by this approach, a low and high retreat scenarios is defined as the trajectories with the 25th and 75th percentile retreats at 2100.

~~Result in the retreat is up to 15 km by 2100 in RCP8.5-Rmed scenario (?). In the following, these retreat scenarios are termed Rlow, Rmed and Rhigh (Tab. 2). The retreat mask for RCP8.5-Rhigh in 2100 is exemplary exemplarily shown in Fig. 4b. Please note, that within this method, the calving front retreat is directly prescribed and no longer a response of the ISM (i. e., not a result of ice velocity at calving front, calving rate and frontal melt). The imposed retreat is therefore a composition of ice discharge, calving and frontal melt. the future projection experiment RCP8.5-Rnone experience no retreat of marine-terminating outlet glaciers.~~

~~The~~

2.5 Comparability of experiments

A central question about resolution dependence is always "How comparable are the results?" and "What is controlling the results?". The presented initialization procedure and involved parameters are achieved for the high-resolution simulations (G750). The simulations with a coarser resolution would probably require other parameters, e.g. to obtain a better result to observational targets or to achieve a reduced model drift. However, we decided here to keep model parameters (e.g. inversion parameters) and parameterizations (e.g. sub-grid scheme at grounding line) unchanged for all simulations. Similarly for the retreat masks, we rely on binary retreat masks for all adopted resolutions although the ISMIP6 protocol recommends using requests a sub-grid scheme to simulate fractional retreat in a grid cell for coarse resolution models. The ISMIP6 AWI-ISSM contribution are performed without fractional retreat, and therefore the additional conducted simulations in this study equivalently do not use a sub-grid scheme. This enables a consistent comparison between the different grids and test their sensitivity to grid resolution. Moreover, a sub-grid scheme would mimic a higher resolution which is not wanted here. However, the binary retreat masks (i.e. ice and non-ice covered cells) are interpolated to the native grid by nearest neighbour interpolation. Retreat occurs once a cell is fully emptied. On the hand this strategy simply assumes that the results are comparable as they build on the same basis. On the other hand it avoids exploring parameter spaces which are out of the scope of this study.

3 Results

Before presenting the results, we aim to address the terminology used for clarity. Following the glossary in Cogley et al. (2011) ice discharge is computed as the product of ice thickness h and the depth-averaged velocity \bar{v} . In the following, the lower-case q refers to the local ice discharge at a point, and the upper-case Q refers to the glacier-wide quantity (analogous for other quantities such as glacier-wide calving D and local calving d). Quantities at the margin are reckoned in the normal direction. For the geometric input we are following the same strategy. It is always a compromise between matching the observed geometry or being closer to a steady-state. Here, we put more weight on having the initial geometry closer to the observed geometry. Therefore, we directly started the historical run after the inversion and no further relaxation run is performed to bring the model

to a steady-state. As the model is likely not in steady-state at the initial state, we expect a model drift in the transient runs; which would not be the case for models that do a relaxation towards a steady-state after the inversion.

3 Results

3.1 Initial state Historical scenario

345 To evaluate the modelling decisions pertaining the initialization, the state of the ice sheet at the end of the historical period is compared to observations. Due to the sparseness and limited temporal and spatial coverage of available observations, we rely on the BedMachine v3 (150 m grid spacing) and MEASURE ~~datasets~~ data sets (250 m grid spacing) for ice thickness and surface velocity, respectively. As these data are used in the data assimilation and inversion, velocity and thickness are not independent quantities. However, during the historical period the ice sheet state is altered by the boundary conditions and external forcing.
350 Therefore, the following evaluation attempts to quantify differences from the model configurations at the ISMIP6 projection start date.

Since the results are qualitatively similar for each grid simulation ~~;~~ (Figs. S1, S2 and S3), the surface velocity field of the G750 simulation is exemplarily shown in Fig. 5a. A consequence of the employed basal friction inversion is the high fidelity in simulating the observed velocity field indicated by a low root mean square error (RMSE) (not shown). ~~The evaluation to observed velocities is shown in~~ Fig. 5b. ~~With~~ Notable is the decreasing RMSE with increasing spatial resolution, the root mean square error (RMSE) decreases. At the end of the historical experiment the RMSE is increased compared to the initialization due to geometric and velocity adjustments over the course of the experiment. However, the ice sheet-wide RMSE of each model version is very similar but in the areas of fast-flowing outlet glaciers (observed velocity $> 200 \text{ m a}^{-1}$) differences are more evident: The G4000 and G750 simulations yield ~~RMSE = 150 m a⁻¹ and RMSE = 80 m a⁻¹~~ RMSE = 150 m a⁻¹ and RMSE = 80 m a⁻¹, respectively. Note that these values are not identical to those given in Goelzer et al. (2020), as the evaluation here is based on a different subsampling method. A mean signed difference (MSD) reflects an increasing a stronger underestimation of the simulated velocities with decreasing coarser resolution. The underestimation of prominent outlet glaciers for the G4000 setup is demonstrated in the spatial pattern of velocity differences ~~in~~ (Fig. S1S4). With increasing resolution, the difference pattern becomes more heterogeneous. Although barely visible, the
365 G750 setup provides an interesting signature at narrowly confined outlet glaciers: Generally, the velocities in the main trunk are underestimated while beneath the shear margin velocities are overestimated. This is might be due to the fact, that the employed resolution is not able to resolve the sharp velocity jump across the shear margin.

A similar evaluation for the thickness is performed. The ice sheet-wide RMSE of ice thickness ~~is shown (Fig. 5c) and depicts the same~~ depicts the qualitative similar grid-dependent behaviour as the velocity evaluation ~~(Fig. 5c)~~. Similarly, the
370 RMSE show larger differences in the fast-flow fast-flow regions: The G4000 and G750 simulations yield ~~RMSE = 126 m and RMSE = 45 m~~ RMSE = 126 m and RMSE = 45 m, respectively. In this region, the MSD indicates underestimation of ice thicknesses with increasing resolution. Similar as mentioned above, these values are not identical to those given in Goelzer et al. (2020)

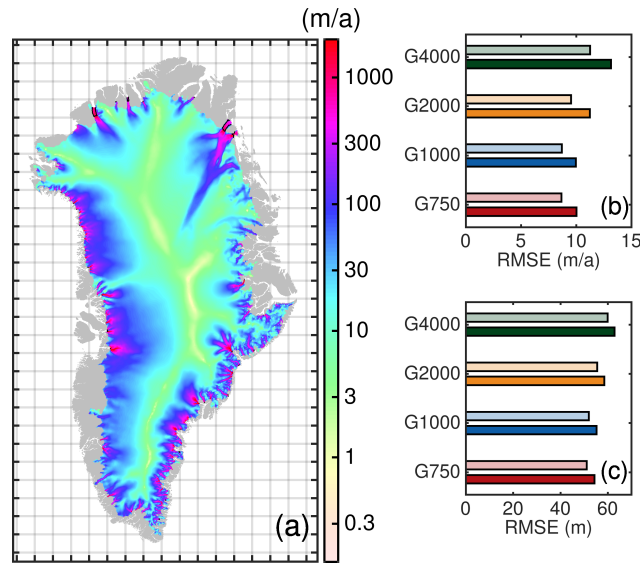


Figure 5. Simulation [results](#) and error estimate of model output at the end of the historical run compared to observations. (a) Simulated surface velocity of the GrIS (m a^{-1}) from the G750 simulation. The grey silhouette shows the Greenland land mask from BedMachine v3. [Thin black lines show the grounding line.](#) (b) Root mean square error (RMSE) of the horizontal velocity magnitude compared to MEASURE. (c) RMSE of ice thickness ([not corrected with ctrl](#)) compared to BedMachine v3. [In \(b\) and \(c\), light and dark colors represent diagnostics at the initialization and end of the historical experiment, respectively.](#) The diagnostics have been calculated on the regular MEASURE and BedMachine grids, respectively.

~~as the evaluation here is based on a different subsampling method.~~ [coarser resolution.](#) Spatial patterns of the thickness differences [over the course of the historical experiment](#) are shown in Fig. [S2S5](#).

375 The stored volumes, ice extent and spatially integrated SMB is among all grid simulations [similar \(\$V = 7.28 \text{ m SLE} \pm 0.2\%\$, \$A = 1.787 \times 10^6 \text{ km}^2 \pm 0.7\%\$, \$\text{SMB} = 375 \text{ Gt a}^{-1} \pm 0.2\%\$ \)](#) rather similar ([\$V = 7.28 \text{ m SLE} \pm 0.2\%\$, \$A = 1.787 \times 10^6 \text{ km}^2 \pm 0.7\%\$, \$\text{SMB} = 375 \text{ Gt a}^{-1} \pm 0.2\%\$](#)). However, the underestimation of velocities and ice thicknesses in the coarser resolution models is confirmed by the temporal mean of the ice discharge in the historical period. The intrinsically simulated ice discharge Q yields 207 Gt a^{-1} to 341 Gt a^{-1} for the G4000 and G750 simulations, respectively. ~~As the ice front is not moving ice discharge~~
 380 ~~Q equals calving D .~~

3.2 Sea-level contribution

In the following the transient effect of spatial resolution on ice volume evolution for the future-climate experiments is studied. The change in ice mass loss is expressed as sea-level contributions. Therefore, the simulated volume above flotation is converted into the total amount of global sea-level equivalent by assuming a constant ocean area of ~~$3.618 \times 10^8 \text{ km}^2$.~~ [\$3.618 \times 10^8 \text{ km}^2\$.](#)

385 [In the following, the mass losses in the projection experiments are corrected with the ctrl run with respect to the reference time.](#)

Table 3. Modelled mass change (mm SLE) in future experiments for all experiments.

<u>Experiment label</u>	<u>G4000</u>	<u>G2000</u>	<u>G1000</u>	<u>G750</u>
<u>corrected with ctrl:[†]</u>				
<u>RCP8.5-Rlow</u>	<u>118.3</u>	<u>119.7</u>	<u>118.6</u>	<u>118.7</u>
<u>RCP8.5-Rmed</u>	<u>122.5</u>	<u>125.8</u>	<u>126.4</u>	<u>126.5</u>
<u>RCP8.5-Rhigh</u>	<u>130.8</u>	<u>134.7</u>	<u>136.8</u>	<u>137.2</u>
<u>RCP8.5-Rnone</u>	<u>108.0</u>	<u>105.1</u>	<u>103.6</u>	<u>103.1</u>
<u>OO-Rmed</u>	<u>19.5</u>	<u>26.4</u>	<u>29.3</u>	<u>30.1</u>
<u>OO-Rhigh</u>	<u>28.9</u>	<u>36.7</u>	<u>41.4</u>	<u>42.6</u>
<u>corrected with ctrl_proj:[†]</u>				
<u>RCP8.5-Rlow</u>	<u>115.8</u>	<u>117.6</u>	<u>117.1</u>	<u>117.2</u>
<u>RCP8.5-Rmed</u>	<u>120.0</u>	<u>123.7</u>	<u>124.8</u>	<u>125.1</u>
<u>RCP8.5-Rhigh</u>	<u>128.3</u>	<u>132.6</u>	<u>135.3</u>	<u>135.8</u>
<u>RCP8.5-Rnone</u>	<u>105.5</u>	<u>103.0</u>	<u>101.8</u>	<u>101.4</u>
<u>OO-Rmed</u>	<u>17.0</u>	<u>24.3</u>	<u>27.7</u>	<u>28.7</u>
<u>OO-Rhigh</u>	<u>26.5</u>	<u>34.6</u>	<u>39.9</u>	<u>41.1</u>
<u>ctrl</u>	<u>-28.0</u>	<u>-12.6</u>	<u>-2.5</u>	<u>-1.5</u>
<u>ctrl_proj</u>	<u>-19.1</u>	<u>-8.7</u>	<u>-2.4</u>	<u>-1.9</u>

[†] Numbers for G1000 and G750 are different compared to Goelzer et al. (2020) as they are differently calculated (e.g. considered ocean area, native versus interpolated grid resolution).

For all conducted projection experiments, the determined GrIS mass losses as a function of time are shown in Fig. 6. ~~The mass losses in the projection experiments are corrected with the control run with respect to the reference time and listed in Tab. 3.~~

~~In the constant climate control~~

~~In the ctrl~~ experiment, the ~~model response in the absence of additional forcing is evaluated~~ transient response (thin coloured lines in Fig. 6). ~~The transient response~~ should not be interpreted as a prediction of actual future behaviour, the ~~control-ctrl~~ run rather confirms that each model has achieved a high degree of equilibration, which is reflected with a low rate of volume change. As the initialization states are presumably different across the employed grids, we expect a different response of the ice sheet as it is likely not in equilibrium with the applied SMB and ice flux divergence. The simulated ice mass evolution shows for all models a mass gain for the 111-year ~~control-ctrl~~ experiment ranging between -28 and -2 mm. With increasing resolution, the drift gets smaller and is minimal for the G1000 and G750 ~~simulations~~ simulations. Although projections are corrected with the ~~control-ctrl~~ run, the higher drift needs caution when interpreting the results as it has, e.g. a consequence on the SMB height-elevation feedback. The higher mass gain rates of the coarser resolutions in the ~~control-ctrl~~ simulation are due ~~with to~~ the lower ice discharge rates (see above sect. 3.1). Although the integrated signal in ice mass change is generally small, the spatial patterns reveal an ice thickness imbalance up to hundreds of metres over the ~~control-ctrl~~ period (Fig. 7). Imposing a

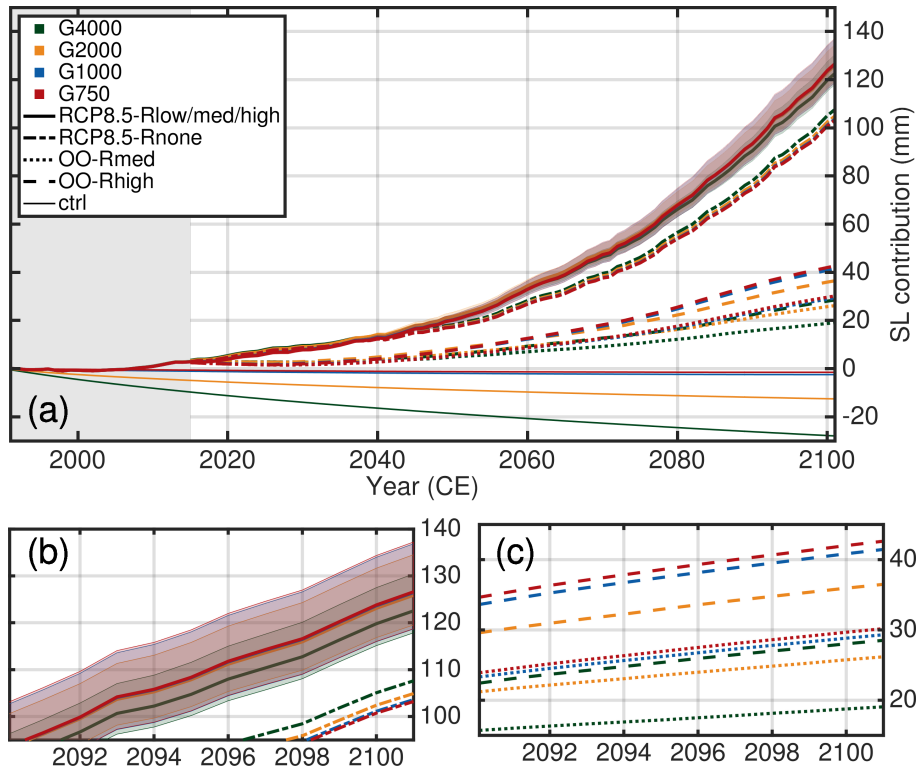


Figure 6. Ice thickness change ($h(t = 2100) - h(t = 2015)$) for the control run. (a) G750 simulation and (b) G4000 simulation. The grey silhouette shows the Greenland land mask from BedMachine v3. Positive values represents thickening, and negative shows thinning. Projected sea-level contribution of the Greenland ice sheet based on MIROC5 RCP 8.5 climate data (a). Coloured lines indicate the different employed grid-resolutions while the individual scenarios are indicated with different line styles. The mass loss trends are corrected with the control-ctrl run (projection-control) relative to the reference time. The grey shaded box shows the historical period. (b) Zoom to the RCP8.5-Rlow/med/high/none scenarios. (c) Zoom to the OO-Rmed/high scenarios.

400 SMB correction to suppress the thickness imbalance would be feasible for maintaining a small drift. However, this is avoided here to enable a clean comparison between the four model version and to leave the ice dynamics some degree of freedom. Moreover, the mass trends represent an important diagnostic. Comparing the ice thickness changes reveal distinct differences between the grid-resolution simulations (Fig. 7). For example, at the end of the control-ctrl run, at some western and north-western locations at the margin the G4000 simulation exhibit thickening while the G750 reveals thinning. Another example is

405 simulated at the south-western margin, where extensive thickening is prevailing in all simulations but reaches farther inland in the coarser resolutions. However, from these figures, it becomes clear that positive and negative thickness changes partially compensate, resulting in a low model drift.

Depending on the projection scenario, the GrIS will lose ice corresponding to a SLE between 19 mm (or 108 excluding OO-Rmed/high) and 137 mm. For the future climate scenarios including atmospheric forcing a gradual increase in mass loss

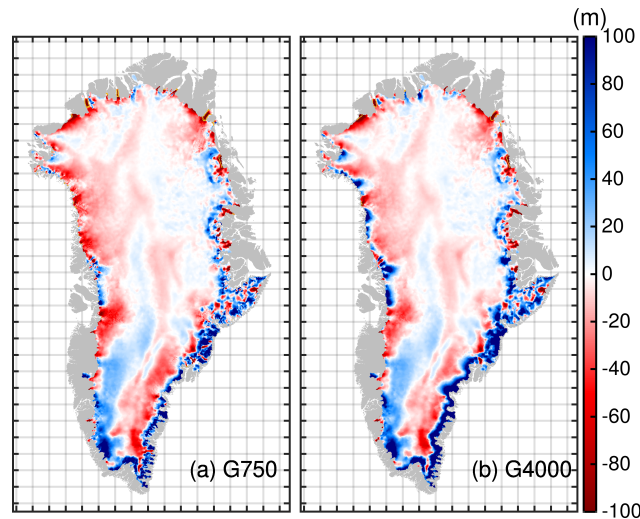


Figure 7. Difference of ice thickness between 2100 and 2015 for the ctrl run. (a) G750 simulation and (b) G4000 simulation. The grey silhouette shows the Greenland land mask from BedMachine v3. Positive values represents thickening, and negative shows thinning. Thin yellow line show the grounding line at the year 2100.

410 until the end of this century is simulated, indicating accelerating mass loss for a high-emission scenario. For the RCP8.5-Rmed the mass loss reaches about 125.3 mm in 2100 (mean over G4000, G2000, G1000 and G750 results). The uncertainty quantification in the oceanic forcing results in a mean sea-level contribution, that is 7.1% less and 5.4% greater for the RCP8.5-Rlow and RCP8.5-Rhigh scenarios, respectively. When no calving front retreat is at play, i.e. the RCP8.5-Rnone scenario, the projected mean mass loss is approx. 105.0 mm, i.e. ~ 20 mm less compared to RCP8.5-Rmed. In contrast, the mean mass loss

415 is considerably reduced to 26 mm and 37 mm in the OO-Rmed and OO-Rhigh experiment, respectively. Interestingly, a linear superposition of RCP8.5-Rnone and OO-Rmed leads to an overestimated mass loss of about 4.1% for G4000 and 5.3% for G750 compared to RCP8.5-Rmed where both external forcings are simultaneously at play; a linear superposition of RCP8.5-Rnone and OO-Rhigh leads to 4.5% and 5.8% overestimation. This is inline with earlier studies where this effect was already reported (Goelzer et al., 2013; Fürst et al., 2015)

420 Among all future projections a resolution-dependent impact on sea-level contribution is generally small compared to the total signal for our grids. In 2100, the spread in sea-level contribution is 6.4 mm in RCP8.5-Rhigh, 4.1 mm in RCP8.5-Rmed, 1.5 mm in RCP8.5-Rlow and 5 mm in RCP8.5-Rnone. Merely the OO-Rlow/med scenarios exhibits a spread of 10.7 mm and 13.6 mm, respectively, which is in the order of the absolute magnitude. A notable feature for all conducted simulations is, that the sea-level contribution in each individual experiment converges with increasing resolution.

425 Figure 8 summarizes the qualitative behaviour of each experiment as function of grid resolution. Note that the sea-level contribution in each experiment is normalized by its maximum. The finer resolutions tend to produce more mass loss in 2100 ~~except for the RCP8.5-Rnone experiment, but an Rmed/high and OO-Rmed/high experiments.~~ An inverse behaviour is determined for the RP8.5-Rnone experiment. The trend in the RCP8.5-Rlow experiment is not clear. The RCP8.5-Rnone and

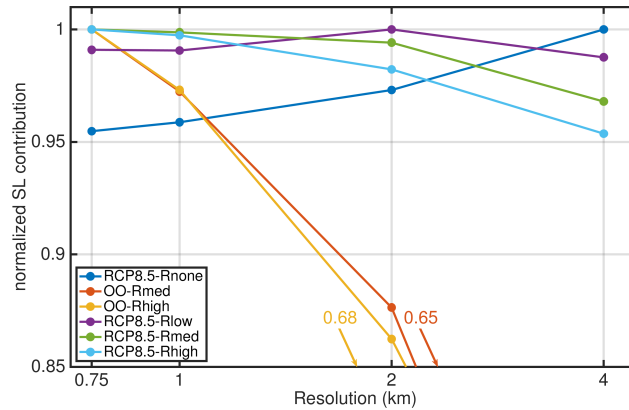


Figure 8. Projected sea-level contribution in 2100 of the Greenland ice sheet as function of the horizontal grid size. Values are normalized to the maximum of each experiment (coloured lines). Note the logarithmic scale of the x-axis.

OO-Rmed/high experiments unveil a linear behaviour as a function of grid size with regression slopes of $m = 1.50 \text{ mm km}^{-1}$, $m = -3.27 \text{ mm km}^{-1}$, and $m = -4.18 \text{ mm km}^{-1}$ respectively. The trend in the full RCP8.5-Rlow/med/high scenarios is not consistent: RCP8.5-Rmed and RCP8.5-Rhigh show a peak in mass loss at the finest resolution, whereby a peak in mass loss is detected-attained in the G2000 simulation for RCP8.5-Rlow. For the latter, it is worth to mention that the variations across the different grid simulations are lesser-less than 1.2%. However, an intriguing effect of the conducted simulations remains the opposite behaviour of the RCP8.5-Rnone and e.g. RCP8.5-Rhigh scenarios. In the following section, we study this effect by analysing the mass partition to get a more in-depth insight into the role of atmospheric and oceanic forcing on grid-resolution.

However, taking into account the inverse grid-dependent behaviour of the RCP8.5-Rnone and OO-Rlow/high scenarios, the combined scenarios demonstrate the competing tendencies of SMB and dynamic contribution. In a particular case, the sea-level contribution is maximized for an intermediate resolution. These competing trends seem to corroborate with results by Achswanden et al. (2019), where an intermediate resolution reveals the largest sea-level contribution. grid-dependent mass loss remains similar when the projections are corrected with the ctrl_proj experiment (Tab. 3).

3.3 Mass partitioning

The relative mass loss partitioning in 2100 is shown in Fig. 9 to explore the role of the grid resolution in each experiment. The bars indicate the relative importance to sea-level contribution of ice dynamic changes in our the projections. The dynamic contribution (composition of front retreat and ice discharge) is calculated as the residual of the total mass change and the integrated SMB anomaly. The remainder explains the part of SMB. The overall picture reveals that for experiments that include the atmospheric forcing the SMB anomaly is the governing forcing regardless of the grid resolutions. However, the importance of the dynamic contribution increases with larger prescribed retreat rates of outlet glaciers; i.e. G750 with RCP8.5-Rhigh on the upper end shows the highest importance of dynamic contribution with up to $\sim 28.4\%$. On the lower end, the RCP8.5-Rnone

450 shows diminished importance of dynamic contribution (<5%). In the OO-Rmed/high scenarios, the mass loss is dominated by dynamic contribution. Concerning the grid resolution, the importance is on an equal level and exceeds 100%. The negative importance of SMB stems from the fact that the glacier retreat is cutting off regions at the ice sheet margin where the static SMB is low.

In the full experiments RCP8.5-Rlow/med/high, an increase in resolution enhances the importance of dynamic contribution. 455 For the G750 simulation it is ~3, 5 and 6% higher for RCP8.5-Rlow/med/high, respectively, compared to G4000. Curiously, the opposite behaviour is observed for the RCP8.5-Rnone experiment, where a finer resolution damps the importance of dynamic contribution; G4000 yield 4.9% whereby G750 2.9% dynamic contribution.

The simulated inverse grid-resolution responses raise the question of the driving causes. Overall the time series of the SMB show a decline and only minor differences among the grid resolutions (Fig. 10a). At the end of the projection, the cumulative 460 SMB is 2.1% and 2.6% lower in the G4000 simulation for RCP8.5-Rnone and RCP8.5-Rhigh, respectively, compared to G750. These differences could be explained by different evolution of ablation areas at the margin and the SMB height-elevation feedback, in particular, affected by the ~~control-ctrl~~ run, among all grid-resolution setups. In contrast, the cumulative ice discharge for these settings reveals an opposing response in the RCP8.5-Rnone and RCP8.5-Rhigh scenarios and more ~~pronounced~~ relative differences between the grid resolutions (Fig. 10b and c). At least for G2000, G1000, and G750, the ice discharge in 465 the RCP8.5-Rnone experiment decreases over the century; the decrease in G4000 is offset by a few decades and exhibits an increase early in the century ~~an increase~~. These reductions explains the grid-dependence of the dynamic contribution as listed in the previous paragraph (RCP8.5-Rnone in Fig. 9). For RCP8.5-Rhigh, the ice discharge shows an increase consistently but is more enhanced in the finer resolutions. This finding corroborates with the grid-dependent increase of the relative ice discharge importance (RCP8.5-Rhigh in Fig. 9). As the opposing differences in RCP8.5-Rnone and RCP8.5-Rhigh are prevailing in ice 470 discharge, it can be concluded that ~~the ice dynamical response~~ resolving ice discharge on the different grids is a decisive factor here. The involved feedback are further explored by focusing on particular outlet glaciers in the next section.

~~However, our grid-dependent results under atmospheric only forcing correlates with the finding in Goelzer et al. (2018, Fig. 1) and the Exp. C2 in Greve and Herzfeld (2013, Figs. 7a and b therein). Interestingly, the causes for the same behaviour seem to have different origins. In Goelzer et al. (2018) the effect is likely due to an overestimated ablation area (see also Goelzer et al., 2019) 475 , whereby in our study the effect is attributed to the dynamic response of the ice sheet. The cause for the grid-dependent behaviour in Greve and Herzfeld (2013) is not specified further. Still, it is worth to mention that they report a much better agreement of simulated to observed surface velocities by increasing the resolution. A drawback in our RCP8.5-Rnone study is certainly, that the calving front remains fixed in space and time, so that outlet glaciers are hindered from adjusting freely to topographic changes.~~

480 ~~Our experiments with considered retreat of outlet glaciers could not be compared to the additional scenarios S1, M2 and R8 experiments in Greve and Herzfeld (2013). On the one hand the external forcing approach differs and on the other hand a grid-dependent behaviour in Greve and Herzfeld (2013) is not clear (except for the enhanced sliding experiment S1, where the higher resolution setups show a higher response).~~

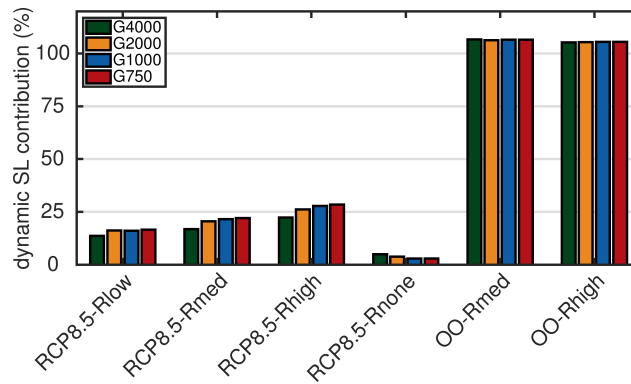


Figure 9. Mass loss partitioning for the conducted experiments. The bars indicate the relative dynamic sea-level contribution to sea-level, calculated as the residual of total the mass change and the integrated SMB anomaly. The dynamic-residual is a composition of front retreat and dynamic responseice discharge.

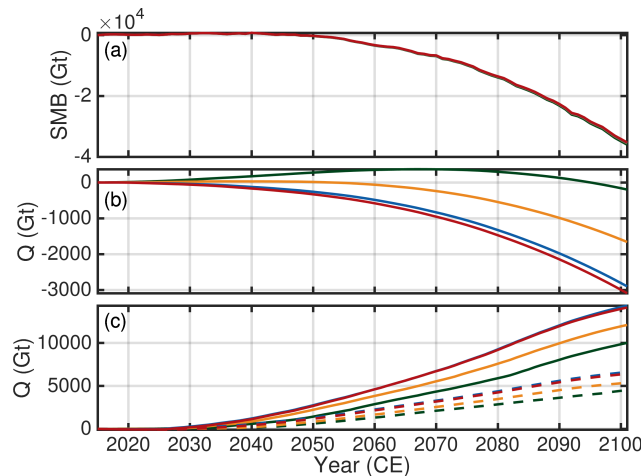


Figure 10. Time series of cumulative SMB anomaly and cumulative ice discharge Q . Colour scheme is as in previous figures. (a) Cumulative SMB anomaly for RCP8.5-Rnone. (b) Cumulative ice discharge Q for RCP8.5-Rnone. (c) Ice discharge for RCP8.5-Rhigh (solid lines) and RCP8.5-Rlow (dashed lines). Cumulative SMB anomaly for RCP8.5-Rhigh and RCP8.5-Rlow is qualitatively similar to RCP8.5-Rnone. Ice discharge is not corrected with the control-ctrl run.

3.4 Outlet glacier response

485 The fact that the centennial mass loss for the full experiments increases as the grid size reduce-reduces raises the question whether this is caused by ice dynamics alone, dominant feedback with surface mass balance or the retreat, or other not-obvious factorsome-into-playnon-obvious factors. We conduct an in-depth analysis of numerous prominent outlet glaciers at GrIS (Fig. S3-S6 and table with analysis provided as separate-separate SI). The general-picture-reveals-the-responses-of-most-of-the

outlet glacier reveal the deduced grid-dependent behaviour ~~, i.e. where~~ higher resolutions cause an enhanced discharge. This
490 is exemplary illustrated in Fig. 11a for Helheim Glacier. However, this behaviour could not be adopted to all selected outlet
glaciers. The presented example demonstrates that the bed-bedrock topography deviates significantly among the different grid-
resolutions. Generally, the bed-bedrock topography of the coarser resolution is located above the bed from the finer resolution.
This topographic effect is restricted to narrow confined outlet glaciers that obey a characteristic width in the order of a few
kilometres. Outlet glaciers that have a larger characteristic width, such as Humboldt glacier, reveal in our setups a comparable
495 bed-bedrock topography. These glaciers seem to have a qualitatively equal behaviour for glacier speed-up and change in ice
discharge for all employed grid resolutions (Fig. 11b). This analysis demonstrates that adjacent glaciers that experience similar
environmental conditions may behave differently because ice discharge is strongly controlled by glacier geometry.

~~The grid-dependent behaviour is highly connected to the bed topography. To study whether the response behaviour is an
effect by purely reducing the grid size, we repeated the OO-Rhigh and RCP8.5-Rhigh experiments with a G1000 simulation
500 that uses re-gridded bed topography and friction coefficient from the G4000 initial state (not shown). Projected sea-level
contributions by this setups are closer to the G4000 simulation and therefore demonstrate the reduction of sea-level contribution
by omitting detailed information from higher resolution. Consequently, these simulations confirm that in our setup a driving
mechanism for the grid-dependent behaviour stems from additional information in the input data.~~

Glaciers that are converted from a ~~marine-terminating to a land-terminating~~ marine-terminating to a land-terminating glacier
505 by retreating out of the water build an own class. These glaciers are no longer subject of the retreat and show a collapse in ice
discharge regardless of the grid resolution as illustrated for Store Glacier in Fig. 11c. The qualitative behaviour of the retreat
seems to be similar as reported in Aschwanden et al. (2019, Fig. 4b therein), but the timing of the retreat is different. In our
study, Store Glacier is unstable and retreats within this century out of the water, while in Aschwanden et al. (2019) Store Glacier
is in a very stable position; the quick retreat sets in far beyond 2100 once the glacier loses contact with the bedrock high. This
510 different response is related to the employed retreat parametrization that lacks information of the bedrock topography, such as
topographic highs and lows.

~~For the scenarios with considered outlet glacier retreat, the induced surface lowering and frontal perturbations cause larger
thinning rates and glacier acceleration; together an increase in ice discharge~~ The RCP8.5-Rnone shows a distinct slow-down
in ice velocities as illustrated in Fig. 11d for Store glacier. Visible is a larger slow-down of the higher resolutions; the same
515 behaviour holds for the ice discharge q . This is in-line with the finding above, that the scenario RCP8.5-Rnone reveals reduced
ice discharge (Fig. 10b).

4 Discussion

The simulations presented here show that the projected sea-level contribution is sensitive to the spatial resolution. The sensitivity
effect depends on the climate forcing, with oceanic and atmospheric forcings showing opposite and non-trivial responses. The
520 simulations have turned out that the ice discharge to the ocean is a decisive factor here controlling the grid-dependent spread.
As shown above, outlet glaciers respond differently to external forcing, dependent on the employed grids and geometrical

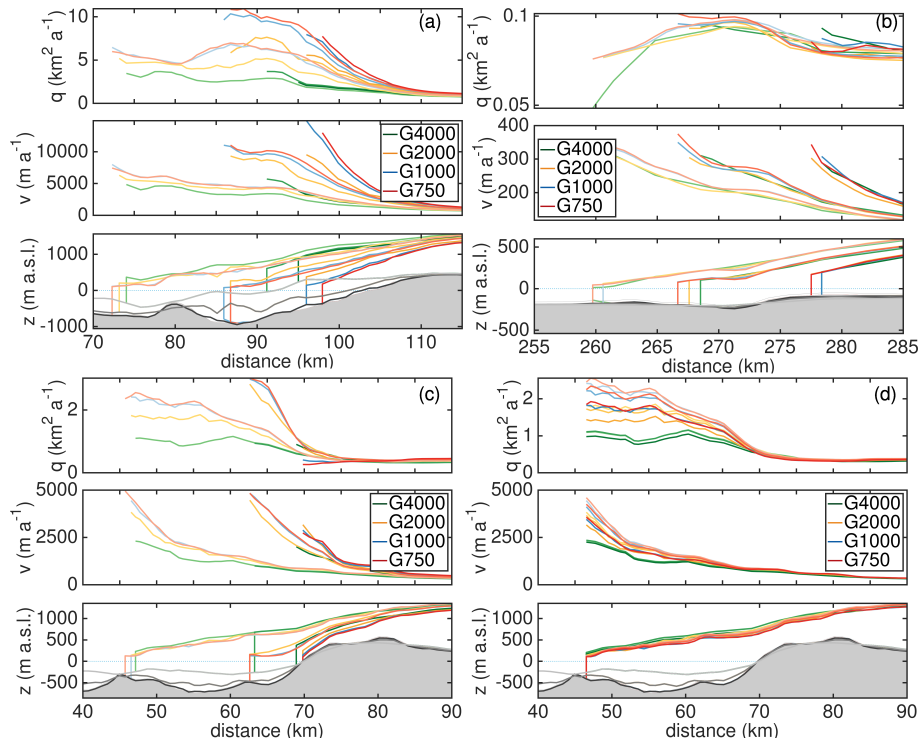


Figure 11. Response of outlet glaciers. Colour scheme is the same as in previous figures and light to dark colours indicate the years 2015, 2070 and 2100. (a) Helheim Glacier under RCP8.5-Rhigh forcing. (b) Humboldt Glacier under RCP8.5-Rhigh forcing. (c) Store Glacier under RCP8.5-Rhigh forcing. (d) Store Glacier under RCP8.5-Rnone forcing. Upper rows show the transient behaviour of the ice discharge q , the middle rows the surface velocity v and lower rows the evolution of the ice geometry. In the lower rows, the grey shaded area depicts the bedrock topography from the G750 simulation. The grey lines from dark to light indicate the bedrock topography from the G1000, G2000 and G4000 simulation. None of the quantities are corrected with the ctrl run. Distance is relative to an arbitrary point.

setting. In such a non-linear system examining a driving mechanism remains challenging. However, despite the somewhat heterogeneous response of outlet glaciers the different scenarios tend to produce an overall trend in characteristic fields that explains the different responses.

525 The different responses in the full scenarios could be attributed to the ability to resolve bedrock topography and the interaction with basal sliding. Figure 12 illustrates spatial changes in the effective pressure and basal sliding velocity for RCP8.5-Rhigh. A common characteristic for G750 is a stronger decrease in effective pressure, which is concentrated in areas where the finer grid shows a deeper bed of the marine portions compared to G4000. Due to the linear dependence of τ_b on effective pressure (Eq. 1), basal sliding velocities increase stronger in the finer resolution. This feedback is enhanced as the
530 SMB perturbations lead to a decrease in ice thickness, hence in a decrease of the effective pressure. The transient evolution reveals that thinning and acceleration have a larger imprint in the finer resolution by propagating faster and further that thinning and acceleration propagate faster and farther upstream in the inland finer resolution. The higher signal propagation

rates may have additional consequences on longer time scales as the surface melt is amplified by the positive surface mass balance-elevation feedback exposing the ice surface to higher air temperatures.

535 ~~The distinct slow-down in~~ It remains questionable, if the widespread glacier acceleration is induced by the frontal stress perturbation instead of the decrease in the effective pressure. To isolate this effect we conduct a RCP8.5-Rnone ~~is reflected in the outlet glacier response as illustrated in~~-Rhigh simulation (not shown) where the effective pressure is held constant to the historical level. This setup reveals a very limited acceleration of a few glaciers in the G4000 simulation; some show no response or even a slow-down. In the corresponding G750 simulation most of the outlet glaciers show a speed-up but this effect
540 is very localized and do not reach far upstream. Therefore, we conclude, that the pronounced decrease of the effective pressure along with the acceleration of outlet glacier is a dominant mechanism controlling the grid-dependent spread.

In order to investigate whether the response behaviour is an effect by purely reducing the grid size, we repeated the OO-Rhigh and RCP8.5-Rhigh experiments with a G1000 simulation using re-gridded bedrock topography and friction coefficient from the G4000 initial state (simulations are not shown). This setup adopts a high-resolution grid but omits detailed information from the
545 high-resolution input data. Projected mass loss by this setups is closer to the G4000 simulation. They, therefore, demonstrate that a high model resolution alone is insufficient to explain the grid-dependent sea-level contribution. As a consequence, a driving cause for the grid-dependent behaviour arises from additional information in the input data. Therefore, we conclude that the grid-dependent behaviour is highly connected to the bedrock topography because the different models represent the bedrock topography quite differently.

550 Compared to the full and ocean only scenario, the atmospheric only scenario unveils a stronger mass loss for the coarse resolution. To some extent, this could be explained by a slightly lower SMB in the coarser resolution. However, the finer resolution produce a stronger reduction of ice discharge over the course of the experiment. Although for many of the outlet glaciers the effective pressure decreases (not as strong as for the scenarios with considered retreat), there is instead a slowdown of most glaciers (Fig. 11d for Store glacier. Still visible is the larger slow-down of the higher resolutions. We attribute this
555 different response to the changing driving stress^{13c,d}). Again, these differences are concentrated in areas where the finer grid shows deeper troughs. Curiously, the finer resolution is better able to resolve these details, but the velocity evolution causes an extra reduction in ice discharge compared to coarser resolution. This non-trivially response is illustrated with the change in driving stress, approximated as $\tau_d = \rho_i g h |\text{grad} z_s|$ (Fig. S18^{13a,b}). Compared to 2015, the driving stress has decreased slightly locally decreased more in the higher-finer resolution in 2100 (e. g., north-western margin); or even show an opposite trend
560 (e. g., south-eastern margin). However, the changed driving stress interact with adjusted basal drag. The effect of resolution influences the sliding velocity in a twofold way: inversions for each resolution setup result in different k^2 , as the geometric component in N differs with resolution. By analysing atmospheric-only simulations (compared to the coarser resolution; away from the marginal region, the driving stress changes are on a comparable magnitude for all employed grids. These results indicate that the reduction of the effective pressure is outperformed by geometric adjustments in the RCP8.5-Rnone)-we find
565 that scenario. This experiment intended to omit an interaction of the glacier with a changing ocean forcing, but the assumption of a fixed calving front hinder outlet glaciers from adjusting freely to topographic changes. They, therefore, do not experience reduced buttressing or frontal stress perturbations which are necessary mechanisms to trigger widespread glacier acceleration

(e.g. Bondzio et al., 2017). In future studies, it might be desirable to allow the calving front to adjust although the oceanic forcing is held constant. Nevertheless, the simulations indicate that without a frontal stress perturbation an ensuing speed-up of the outlet glacier is not initiated. This highlights the importance for capturing calving events, i.e tracking the ice front position in numerical models, most accurate.

The inverse grid-dependent behaviour of the evolution of SMB, results in a larger reduction in N and τ_b , as well as decreasing sliding velocity for higher resolutions. In all scenarios, nearly all glaciers respond to lower N with higher resolutions. The change in driving stress is potentially responsible for the strong variation in τ_b . However, this needs further investigation. Beside these competing stresses, find that RCP8.5-Rnone and OO-Rmed/high scenarios have some implications when interpreting the mass loss of the ice sheet. The combined scenarios demonstrate that in a particular case, the sea-level contribution is maximized for an intermediate resolution. Depending on the horizontal grid resolution, the change in τ_b and τ_d is very pronounced in and around the main trunks (see competing tendencies of SMB and ice discharge are differently resolved. This finding seems to corroborate with results by Aschwanden et al. (2019), where an intermediate resolution reveals the largest sea-level contribution.

A convergence of the grid-dependent estimates of sea-level contribution emerges around $RES_{\text{high}} \leq 1 \text{ km}$. This value corroborates with Aschwanden et al. (2016) for capturing outlet glacier behaviour indicating an upper limit for horizontal grid resolution. However, the converging behaviour should be treated with some caution. We cannot exclude whether a model resolution finer than 750m would lead to results that deviate from the convergence. On the one hand, the 150 m horizontal grid spacing of the BedMachine v3 data set is much finer than our finest resolution of 750 m. As the retreat parametrization is insensitive to bed undulations, resolving the outlet glacier cross-sections is important for accurately model ice discharge. Since the glacier cross-sections are reasonable well approximated in G750, we do not expect that a resolving the geometry higher would drastically alter ice discharge rates. On the other hand, there are indications that at a resolution of 750 m the HO solution is not fully converged (Pattyn et al., 2008). Adopting a higher resolution could have implications for the ice flow, and hence for the evolution of ice discharge. Likewise, in Aschwanden et al. (2019, Fig. S4 therein), the ice discharge is shown to increase as the mesh resolution is increased, and seem to converge below a resolution of $\leq 1800 \text{ m}$. However, the finer resolutions of 450 and 600 m seem to produce again a somewhat lower ice discharge. That might indicate that the underlying processes are not fully converged and still causing changes in mass loss trends.

Our grid-dependent results under atmospheric only forcing correlates with the finding in Goelzer et al. (2018, Fig. 1) and the Exp. C2 in Greve and Herzfeld (2013, Figs. 7a and b therein). Interestingly, the causes for the same behaviour seem to have different origins. In Goelzer et al. (2018) the effect is likely due to an overestimated ablation area (see also Goelzer et al., 2019), whereby in our study the effect is attributed to the change in ice discharge of the ice sheet. The cause for the grid-dependent behaviour in Greve and Herzfeld (2013) is not specified further. Still, it is worth mentioning that they report a much better agreement of simulated to observed surface velocities by increasing the spatial resolution. Our experiments with the considered retreat of outlet glaciers could not be compared to the scenarios S1, M2 and R8 experiments in Greve and Herzfeld (2013). On the one hand, the external forcing approach differs. On the other hand, a grid-dependent behaviour in Greve and Herzfeld (2013) is not clear (except for the enhanced sliding experiment S1, where the finer resolution setups show a higher response).

Besides the fixed calving front in the atmospheric only scenario, further limitations of our study must be noted. The spread of projected sea-level contribution among all grids is likely subject to the chosen type of friction law. The choice of the basal friction law used in ISMs remains a matter of debate (Stearns and van der Veen, 2018; Minchew et al., 2019) and a potential source of uncertainty in sea-level projections (e.g. Brondex et al., 2019). Compared to our used type of friction law, there are some indications that friction laws satisfying an upper bound for the basal drag are more reliable (e.g. Schoof, 2005; Gagliardini et al., 2007). In brief, these type of friction laws invoke a switch for the friction regimes (low and high N , respectively) so that the influence of the effective pressure on the basal drag at slow ice flow is vanishing. It would be most interesting to evaluate their sensitivity to the horizontal resolution for projections on centennial time scales.

Another limitation concerns the choice of inversion parameters. We performed the inversions for basal parameters for each grid resolution individually but relying on the inversion parameters tuned for the high-resolution setups. Effectively, this results in an overall comparable pattern for the flow velocities (Fig. S17 and 18). This exemplifies the need for resolving the shear margins particularly high, which we have not accomplished in this study. S1 and S2) and basal friction coefficient (Fig. S3) for all grids. However, on smaller scales, the inversion approach produces significantly different k^2 in many glacier basins. Recalling the relationship between N and k^2 , these different patterns are plausible but could potentially be a result from non optimal inversion parameters. However, this different spatial patterns might an additional contribution to the grid dependence of the simulations. In future studies, it will be worth investigating this influence only, e.g. by tuning the inversion parameters for each grid separately to find the optimal parameters.

Response of outlet glaciers. Colour scheme is the same as in previous figures and light to dark colours indicate the years 2015, 2070 and 2100. (a) Helheim Glacier under RCP8.5-Rhigh forcing. (b) Humboldt Glacier under RCP8.5-Rhigh forcing. (c) Store Glacier under RCP8.5-Rhigh forcing. (d) Store Glacier under RCP8.5-Rnone forcing. Upper rows show the transient behaviour of the ice discharge q , the middle rows the surface velocity v and lower rows the evolution of the ice geometry. In the lower rows, the grey shaded area depicts the bedrock topography from the G750 simulation. The grey lines from dark to light indicate the bedrock topography from the G1000, G2000 and G4000 simulation. Ice discharge and geometry is not corrected with the control run.

5 Discussion

However, the simulations conducted here reveal a grid-dependent spread in the RCP8.5-Rlow and RCP8.5-Rhigh full scenarios ranging between 1.2 and 5.3%. The, which is of comparable magnitude as the surface mass balance-elevation feedback (Eq. 4). The latter is recognized as an important mechanism and accounts for an additional sea-level contribution of about 6-8% (Goelzer et al., 2020) which is of comparable magnitude. A feedback that we have not considered, but likely cause further increase in sea-level contribution and associated grid-dependent spread, is the enhanced surface melt influencing the basal conditions. Subglacial hydrology model have shown the localised effect on N , which is likely having consequences on the spread between the employed grid resolutions (e.g. Werder et al., 2013; de Fleurian et al., 2016; Sommers et al., 2018; Beyer et al., 2018)

635 =

The inferred basal friction coefficient k^2 applies to basal properties for the present-day state, and its distribution is driven by our capability to have a decent distribution of N , as the inversion strongly affected by that. Given that we rely on the parameterisation $N = \rho_w g h + \min(0, \rho_w g z_b)$, we may suppress dynamic responses and greatly simplify the representation of N , the effect of a reorganization of basal conditions (in either way). That might explain the frequently detected behaviour, that velocities at retreating glacier fronts remain at a similar level. This can be overcome only with or the effect of increased availability of water due to increasing surface melt on basal sliding is suppressed. To overcome this limitation, an adequate subglacial hydrology model could be invoked, even if not considering seasonality. In this study, we performed the inversions for basal parameters for each grid resolution individually, which resulted in significantly different k^2 in many glacier basins. This different spatial pattern is an additional contribution to the grid dependence of the simulations. In future studies Subglacial hydrology model has shown the localized effect on N , which is likely having consequences on the spread between the employed grid resolutions (e.g. Werder et al., 2013; de Fleurian et al., 2016; Sommers et al., 2018; Beyer et al., 2018).

A feedback that is not fully covered in our simulations is shear margin weakening and its influence on the evolution of flow velocities. Although the shear margins are weakly developed in the simulations (more pronounced in the finer resolutions), it is worth to investigate this influence isolated. Also other studies highlight the effect of sliding on sea-level projections (e.g. Brondex et al., 2019), underpinning the importance of this mechanism.

However, our grid-dependent estimates of sea-level contribution converges around $RES_{\min} \leq 1$ km. This value corroborates with Aeschwanden et al. (2016) for capturing outlet glacier behaviour indicating an upper limit for horizontal grid resolution. Although we have already a decent resolution in G750, we recognise, that in many of the narrow fjords, the resolution is still insufficient, expected that a thermo-mechanical coupling could further weaken the shear margins as a response to frontal stress perturbations (e.g. Bondzio et al., 2017). Such a coupling would increase the widespread inland flow acceleration and enhances the rate of mass loss. However, the change in τ_b and τ_d is very pronounced in and around the main trunks and quite differently for the adopted grids (see Fig. S20 and 21). These patterns exemplify the need for resolving the shear margins particularly high, which we have not fully accomplished in this study as shear margins are becoming, in numerous cases subgrid-, sub-grid phenomena. This may be a reason for under-representing glacier velocities inside the main trunk and over-estimate velocities outside the main flow as apparent in G750. This effect shall be addressed in further studies, in which ideally error estimators as presented by dos Santos et al. (2019) are engaged higher resolutions are employed or error estimators are engaged (e.g. dos Santos et al., 2019).

It would be most interesting to evaluate the effect the ocean does have on mass loss in general, assessing the importance of it. In our opinion, such an assessment needs to be based on simulations that represent the current dynamics of the glaciers particularly well, as the outcome depends on the capability of the model to capture the real dynamic response. Given that many of outlet glaciers exhibit lower velocities in the main trunk than observed, we thus do not draw any conclusion on the impact and importance of oceanic induced ablation versus SMB, as we lack significant feedback mechanisms (e.g., seasonal lubrication and its evolution until 2100).

~~The floating tongues of Ryder Glacier, Petermann Glacier and Nioghalvsfjersbræare thinning to the minimum thickness. They would retreat further, if not forced to their positions by the retreat method applied here. This may limit acceleration, and consequently, our simulations likely miss a speed-up caused by the loss of the exerted buttressing of these floating tongues.~~

5 Conclusions

We applied the three-dimensional finite-element higher-order model ISSM to the Greenland ice sheet to simulate the future response under climatic changes specified by the ISMIP6 protocol. The sensitivity of mass changes to the spatial resolution is tested by employing four different grids with varying horizontal resolution ranging from 4 to 0.75 km at fast-flowing outlet glaciers. The simulations reveal up to $\sim 5.3\%$ more sea-level rise compared to the coarser resolution in the full scenario RCP8.5-Rhigh and $\sim 3.2\%$ for RCP8.5-Rmed. In scenarios where a change in SMB is omitted, and only outlet glacier retreat is at play, the finer resolutions produce significantly more mass loss (up to 33%). When no retreat is enforced, the sensitivity of the grid-dependence exhibits an inverse behaviour, i.e. the coarser resolutions produce more mass loss. This finding is important to recognise for ice sheet models that have SMB as the dominant mass loss driver.

~~An apparent behaviour at many but not all individual outlet glaciers is the spread of thinning and acceleration farther inland with higher resolution. This, in turn, leads to higher ice discharge and mass transport from the interior to the ocean. The identified key mechanism that is affected by resolution is sliding, as the friction coefficient k^2 (even if static), the effective pressure N and the basal drag τ_b interact individually with the bedrock topography. In general, a reduction of N is overcompensated by a reduction in τ_b , leading to an increase in sliding speed. This study does not include an effect of increased availability of water due to increasing surface melt, thus no lubrication effect, at all. Taking this into account in future studies is important, and it may alter our findings.~~

The results presented underline the importance of resolving the bedrock topography accurately. Areas with simple and low bedrock undulations experience a similar response in all model resolution. In areas with complex and high bedrock undulations striking differences between the employed grids emerge. A mechanism that exerts an important control on the resolution dependent spread is basal sliding predominantly in marine portions of outlet glaciers glacier. Since we rely on a greatly simplified effective pressure parametrization, further work with is needed to prove the robustness of this conclusion.

Given the strong interaction of the bedrock topography with sliding, it is obvious, that the major outlet glacier should be surveyed with the latest radar technology to obtain a substantially improved survey of the ~~base~~bedrock topography, the area of expected retreat and connected areas further upstream. This, in turn, requires ice sheet models ready to resolve these areas in grids and physics adequately.

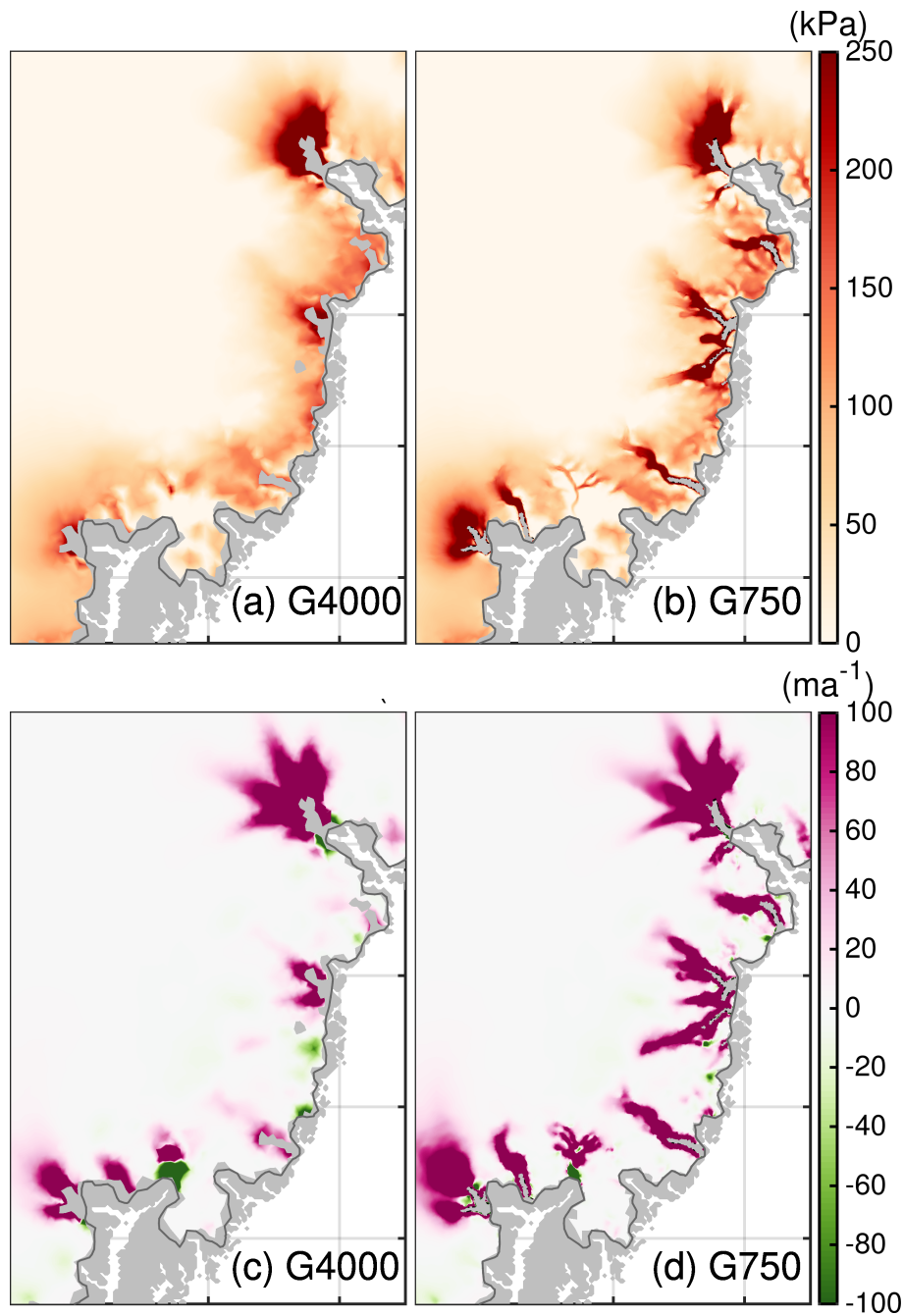


Figure 12. (a,b) Difference of effective pressure between 2100 and 2015 for the southeast region. (c,d) Difference of basal velocity between 2100 and 2015 for the southeast region. Region subsets are shown in See Fig. 2. Dark gray line indicates the initial ice extent. Thin black line indicating the grounding line is not visible as it falls together with the calving front. The grey silhouette shows the Greenland land mask from BedMachine v3.

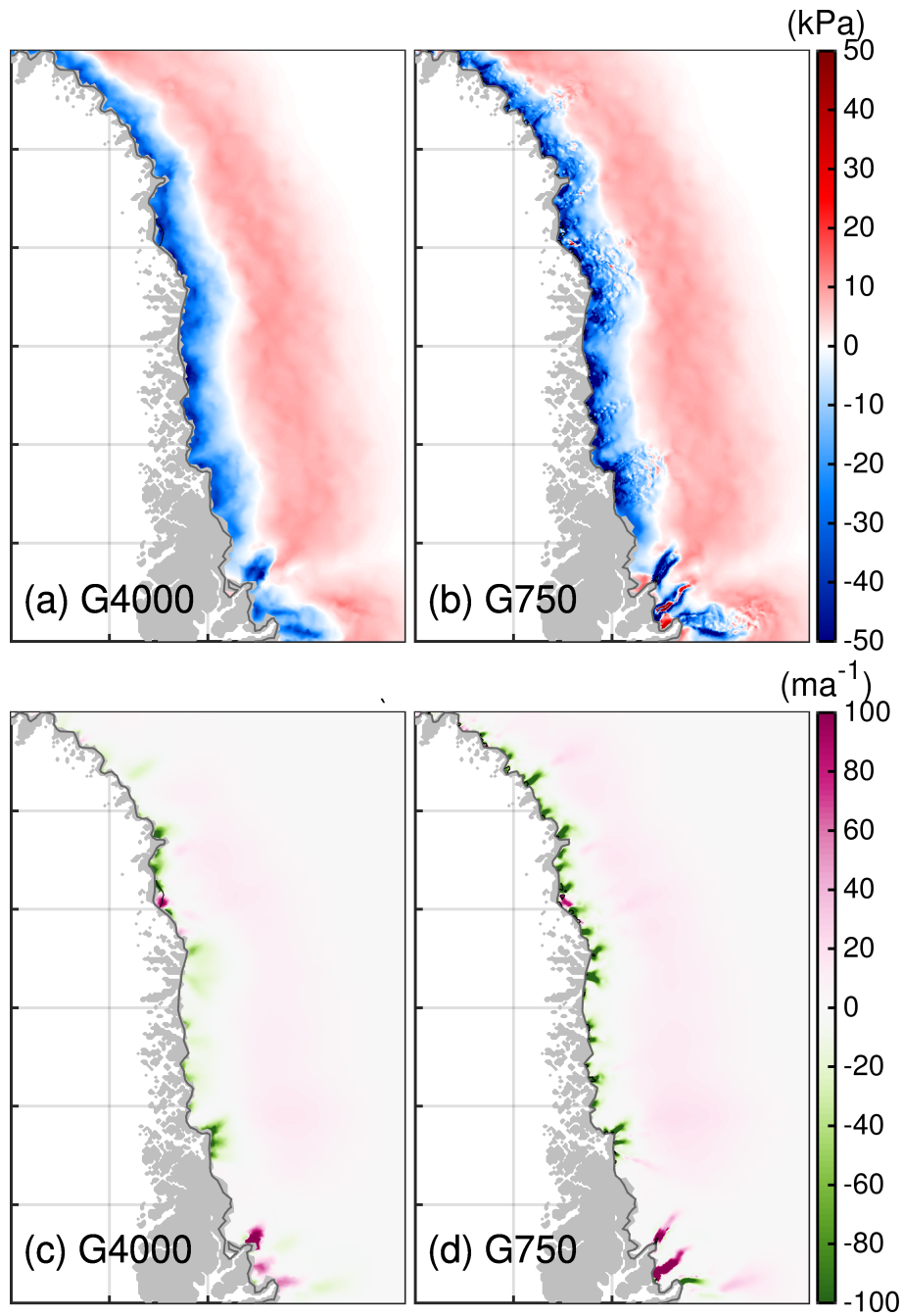


Figure 13. (a,b) Difference of driving stress between 2100 and 2015 for the northwestern region. (c,d) Difference of basal velocity between 2100 and 2015 for the northwestern region. Region subsets are shown in See Fig. 2. Dark gray line indicates the initial ice extent. Thin black line indicating the grounding line is not visible as it falls together with the calving front. The grey silhouette shows the Greenland land mask from BedMachine v3.

Code and data availability. Results on the native grids are available via the PANGAEA (www.pangaea.de) database (<https://doi.pangaea.de/XXX>). The forcing data sets are available through the ISMIP6 wiki and are also made publicly available via <https://doi.org/xxx>. The ice flow model ISSM is open source and freely available at <https://issm.jpl.nasa.gov/> (last access: May 18, 2020), (Larour et al., 2012). Here ISSM version 700 4.16 is used.

Author contributions. MR conducted the study supported by the other authors. MR set up the ISSM model and ran the experiments. AH analysed the results for the individual glaciers. HG calculated the retreat masks. MR wrote the manuscript together with the other authors.

Competing interests. The authors declare that they have no conflict of interest.

Acknowledgements. We thank the Climate and Cryosphere (CliC) effort, which provided support for ISMIP6 through sponsoring of work- 705 shops, hosting the ISMIP6 website and wiki, and promoted ISMIP6. We acknowledge the World Climate Research Programme, which, through its Working Group on Coupled Modelling, coordinated and promoted CMIP5 and CMIP6. We thank the climate modeling groups for producing and making available their model output, the Earth System Grid Federation (ESGF) for archiving the CMIP data and providing access, the University at Buffalo for ISMIP6 data distribution and upload, and the multiple funding agencies who support CMIP5 and CMIP6 and ESGF. We thank the ISMIP6 steering committee, the ISMIP6 model selection group and ISMIP6 ~~dataset~~ data set preparation group for 710 their continuous engagement in defining ISMIP6 and all their efforts.

We thank two anonymous reviewers for their helpful suggestions to improve the manuscript. Martin Rückamp acknowledges support of the Helmholtz Climate Initiative REKLIM (Regional Climate Change). Heiko Goelzer has received funding from the programme of the Netherlands Earth System Science Centre (NESSC), financially supported by the Dutch Ministry of Education, Culture and Science (OCW) under grant no. 024.002.001.

715 We thank Thomas Kleiner (AWI) and Ralf Greve (ILTS) for continuous and fruitful discussions on simulations. We would like to thank Natalja Rakowsky, Malte Thoma and Bernadette Fritsch for maintaining excellent computing facilities at AWI and DKRZ. The high-resolution simulations were run on the DKRZ HPC system Mistral under grant ab1073. We also acknowledge the outstanding support of the ISSM team.

References

- 720 Aschwanden, A., Fahnestock, M. A., and Truffer, M.: Complex Greenland outlet glacier flow captured, *Nat. Commun.*, 7, 10524, <https://doi.org/10.1038/ncomms10524>, 2016.
- Aschwanden, A., Fahnestock, M. A., Truffer, M., Brinkerhoff, D. J., Hock, R., Khroulev, C., Mottram, R., and Khan, S. A.: Contribution of the Greenland Ice Sheet to sea level over the next millennium, *Science Advances*, 5, <https://doi.org/10.1126/sciadv.aav9396>, 2019.
- Barthel, A., Agosta, C., Little, C. M., Hattermann, T., Jourdain, N. C., Goelzer, H., Nowicki, S., Seroussi, H., Straneo, F., and Brace-
725 girdle, T. J.: CMIP5 model selection for ISMIP6 ice sheet model forcing: Greenland and Antarctica, *The Cryosphere*, 14, 855–879, <https://doi.org/10.5194/tc-14-855-2020>, 2020.
- Beckmann, A. and Goosse, H.: A parameterization of ice shelf-ocean interaction for climate models, *Ocean Modelling*, 5, 157–170, [https://doi.org/10.1016/S1463-5003\(02\)00019-7](https://doi.org/10.1016/S1463-5003(02)00019-7), 2003.
- Beyer, S., Kleiner, T., Aizinger, V., Rückamp, M., and Humbert, A.: A confined–unconfined aquifer model for subglacial hydrology and
730 its application to the Northeast Greenland Ice Stream, *The Cryosphere*, 12, 3931–3947, <https://doi.org/10.5194/tc-12-3931-2018>, <https://www.the-cryosphere.net/12/3931/2018/>, 2018.
- Bindschadler, R. A., Nowicki, S., Abe-Ouchi, A., Aschwanden, A., Choi, H., Fastook, J., Granzow, G., Greve, R., Gutowski, G., Herzfeld, U. C., Jackson, C., Johnson, J., Khroulev, C., Levermann, A., Lipscomb, W. H., Martin, M. A., Morlighem, M., Parizek, B. R., Pol-
lard, D., Price, S. F., Ren, D., Saito, F., Sato, T., Seddik, H., Seroussi, H., Takahashi, K., Walker, R., and Wang, W. L.: Ice-sheet
735 model sensitivities to environmental forcing and their use in projecting future sea level (the SeaRISE project), *J. Glaciol.*, 59, 195–224, <https://doi.org/10.3189/2013JoG12J125>, 2013.
- Blatter, H.: Velocity and stress fields in grounded glaciers: a simple algorithm for including deviatoric stress gradients, *J. Glaciol.*, 41, 333–344, <https://doi.org/10.3189/S002214300001621X>, 1995.
- Bondzio, J. H., Morlighem, M., Seroussi, H., Kleiner, T., Rückamp, M., Mouginot, J., Moon, T., Larour, E. Y., and Humbert, A.: The
740 mechanisms behind Jakobshavn Isbræ’s acceleration and mass loss: A 3-D thermomechanical model study, *Geophys. Res. Lett.*, 44, 6252–6260, <https://doi.org/10.1002/2017GL073309>, 2017.
- Brondeux, J., Gillet-Chaulet, F., and Gagliardini, O.: Sensitivity of centennial mass loss projections of the Amundsen basin to the friction law, *The Cryosphere*, 13, 177–195, <https://doi.org/10.5194/tc-13-177-2019>, 2019.
- Budd, W. F., Janssen, D., and Smith, I. N.: A Three-Dimensional Time-Dependent Model of the West Antarctic Ice Sheet, *Annals of
745 Glaciology*, 5, 29–36, <https://doi.org/10.3189/1984AoG5-1-29-36>, 1984.
- Choi, Y., Morlighem, M., Rignot, E., Mouginot, J., and Wood, M.: Modeling the Response of Nioghalvfjærdsfjorden and Zachariae Isstrøm Glaciers, Greenland, to Ocean Forcing Over the Next Century, *Geophysical Research Letters*, 44, 11,071–11,079, <https://doi.org/10.1002/2017GL075174>, 2017.
- Church, J. A., Clark, P. U., Cazenave, A., Gregory, J. M., Jevrejeva, S., Levermann, A., Merrifield, M., Milne, G., Nerem, R., Nunn, P., et al.:
750 Sea level change, in: *Climate Change 2013: The Physical Science Basis. Working Group I Contribution to the Fifth Assessment Report of the Intergovernmental Panel on Climate Change*, pp. 1137–1216, Cambridge University Press, 2013.
- Cogley, J., Hock, R., Rasmussen, L., Arendt, A., Bauder, A., Braithwaite, R., Jansson, P., Kaser, G., Möller, M., Nicholson, L., and Zemp, M.: *Glossary of Glacier Mass Balance and Related Terms*, Tech. Rep. 86, IHP-VII Technical Documents in Hydrology, UNESCO-IHP, Paris, 2011.

- 755 de Fleurian, B., Morlighem, M., Seroussi, H., Rignot, E., van den Broeke, M. R., Kuipers Munneke, P., Mouginot, J., Smeets, P. C. J. P., and
Tedstone, A. J.: A modeling study of the effect of runoff variability on the effective pressure beneath Russell Glacier, West Greenland,
Journal of Geophysical Research: Earth Surface, 121, 1834–1848, <https://doi.org/10.1002/2016JF003842>, 2016.
- dos Santos, T. D., Morlighem, M., Seroussi, H., Devloo, P. R. B., and Simões, J. C.: Implementation and performance of adaptive mesh
refinement in the Ice Sheet System Model (ISSM v4.14), *Geoscientific Model Development*, 12, 215–232, <https://doi.org/10.5194/gmd-760-12-215-2019>, 2019.
- Enderlin, E. M., Howat, I. M., Jeong, S., Noh, M.-J., Angelen, J. H., and Broeke, M. R.: An improved mass budget for the Greenland ice
sheet, *Geophysical Research Letters*, 41, 866–872, <https://doi.org/10.1002/2013GL059010>, 2014.
- Ettema, J., van den Broeke, M. R., van Meijgaard, E., van de Berg, W. J., Bamber, J. L., Box, J. E., and Bales, R. C.: Higher surface
mass balance of the Greenland ice sheet revealed by high-resolution climate modeling, *Geophysical Research Letters*, 36, n/a–n/a,
765 <https://doi.org/10.1029/2009GL038110>, 112501, 2009.
- Eyring, V., Bony, S., Meehl, G. A., Senior, C. A., Stevens, B., Stouffer, R. J., and Taylor, K. E.: Overview of the Coupled Model
Intercomparison Project Phase 6 (CMIP6) experimental design and organization, *Geoscientific Model Development*, 9, 1937–1958,
<https://doi.org/10.5194/gmd-9-1937-2016>, 2016.
- Fettweis, X., Box, J. E., Agosta, C., Amory, C., Kittel, C., Lang, C., van As, D., Machguth, H., and Gallée, H.: Reconstructions of
770 the 1900–2015 Greenland ice sheet surface mass balance using the regional climate MAR model, *The Cryosphere*, 11, 1015–1033,
<https://doi.org/10.5194/tc-11-1015-2017>, 2017.
- Fettweis, X., Hofer, S., Krebs-Kanzow, U., Amory, C., Aoki, T., Berends, C. J., Born, A., Box, J. E., Delhasse, A., Fujita, K., Gierz, P.,
Goelzer, H., Hanna, E., Hashimoto, A., Huybrechts, P., Kapsch, M.-L., King, M. D., Kittel, C., Lang, C., Langen, P. L., Lenaerts, J. T. M.,
Liston, G. E., Lohmann, G., Mernild, S. H., Mikolajewicz, U., Modali, K., Mottram, R. H., Niwano, M., Noël, B., Ryan, J. C., Smith, A.,
775 Streffing, J., Tedesco, M., van de Berg, W. J., van den Broeke, M., van de Wal, R. S. W., van Kampenhout, L., Wilton, D., Wouters, B.,
Ziemen, F., and Zolles, T.: GrSMBMIP: Intercomparison of the modelled 1980–2012 surface mass balance over the Greenland Ice sheet,
The Cryosphere Discussions, 2020, 1–35, <https://doi.org/10.5194/tc-2019-321>, 2020.
- Franco, B., Fettweis, X., Lang, C., and Erpicum, M.: Impact of spatial resolution on the modelling of the Greenland ice sheet surface mass
balance between 1990–2010, using the regional climate model MAR, *The Cryosphere*, 6, 695–711, <https://doi.org/10.5194/tc-6-695-2012>,
780 2012.
- Fürst, J. J., Goelzer, H., and Huybrechts, P.: Ice-dynamic projections of the Greenland ice sheet in response to atmospheric and oceanic
warming, *The Cryosphere*, 9, 1039–1062, <https://doi.org/10.5194/tc-9-1039-2015>, 2015.
- Gagliardini, O., Cohen, D., Raback, P., and Zwinger, T.: Finite-element modeling of subglacial cavities and related friction law, *Journal of
Geophysical Research: Earth Surface*, 112, <https://doi.org/10.1029/2006JF000576>, 2007.
- 785 Gillet-Chaulet, F., Gagliardini, O., Seddik, H., Nodet, M., Durand, G., Ritz, C., Zwinger, T., Greve, R., and Vaughan, D. G.: Greenland ice
sheet contribution to sea-level rise from a new-generation ice-sheet model, *Cryosphere*, 6, 1561–1576, <https://doi.org/10.5194/tc-6-1561-2012>, 2012.
- Gladstone, R., Schäfer, M., Zwinger, T., Gong, Y., Strozzi, T., Mottram, R., Boberg, F., and Moore, J. C.: Importance of basal processes
in simulations of a surging Svalbard outlet glacier, *The Cryosphere*, 8, 1393–1405, <https://doi.org/10.5194/tc-8-1393-2014>, [https://www.
790 the-cryosphere.net/8/1393/2014/](https://www.the-cryosphere.net/8/1393/2014/), 2014.
- Glen, J. W.: The Creep of Polycrystalline Ice, *Proceedings of the Royal Society of London. Series A, Mathematical and Physical Sciences*,
228, 519–538, <https://doi.org/10.1098/rspa.1955.0066>, 1955.

- Goelzer, H., Huybrechts, P., Fürst, J., Nick, F., Andersen, M., Edwards, T., Fettweis, X., Payne, A., and Shannon, S.: Sensitivity of Greenland Ice Sheet Projections to Model Formulations, *Journal of Glaciology*, 59, 733–749, <https://doi.org/10.3189/2013JoG12J182>, 2013.
- 795 Goelzer, H., Nowicki, S., Edwards, T., Beckley, M., Abe-Ouchi, A., Aschwanden, A., Calov, R., Gagliardini, O., Gillet-Chaulet, F., Golledge, N. R., Gregory, J., Greve, R., Humbert, A., Huybrechts, P., Kennedy, J. H., Larour, E., Lipscomb, W. H., Le clec’h, S., Lee, V., Morlighem, M., Pattyn, F., Payne, A. J., Rodehacke, C., Rückamp, M., Saito, F., Schlegel, N., Seroussi, H., Shepherd, A., Sun, S., van de Wal, R., and Ziemen, F. A.: Design and results of the ice sheet model initialisation experiments initMIP-Greenland: an ISMIP6 intercomparison, *Cryosphere*, 12, 1433–1460, <https://doi.org/10.5194/tc-12-1433-2018>, 2018.
- 800 Goelzer, H., Noel, B. P. Y., Edwards, T. L., Fettweis, X., Gregory, J. M., Lipscomb, W. H., van de Wal, R. S. W., and van den Broeke, M. R.: Remapping of Greenland ice sheet surface mass balance anomalies for large ensemble sea-level change projections, *The Cryosphere Discussions*, 2019, 1–20, <https://doi.org/10.5194/tc-2019-188>, 2019.
- Goelzer, H., Nowicki, S., Payne, A., Larour, E., Seroussi, H., Lipscomb, W. H., Gregory, J., Abe-Ouchi, A., Shepherd, A., Simon, E., Agosta, C., Alexander, P., Aschwanden, A., Barthel, A., Calov, R., Chambers, C., Choi, Y., Cuzzone, J., Dumas, C., Edwards, T., Felikson, D.,
- 805 Fettweis, X., Golledge, N. R., Greve, R., Humbert, A., Huybrechts, P., Le clec’h, S., Lee, V., Leguy, G., Little, C., Lowry, D. P., Morlighem, M., Nias, I., Quiquet, A., Rückamp, M., Schlegel, N.-J., Slater, D., Smith, R., Straneo, F., Tarasov, L., van de Wal, R., and van den Broeke, M.: The future sea-level contribution of the Greenland ice sheet: a multi-model ensemble study of ISMIP6, *The Cryosphere Discussions*, 2020, 1–43, <https://doi.org/10.5194/tc-2019-319>, 2020.
- Greve, R.: Relation of measured basal temperatures and the spatial distribution of the geothermal heat flux for the Greenland ice sheet, *Annals of Glaciology*, 42, 424–432, 2005.
- 810 Greve, R. and Herzfeld, U. C.: Resolution of ice streams and outlet glaciers in large-scale simulations of the Greenland ice sheet, *Ann. Glaciol.*, 54, 209–220, <https://doi.org/10.3189/2013AoG63A085>, 2013.
- Iken, A.: The Effect of the Subglacial Water Pressure on the Sliding Velocity of a Glacier in an Idealized Numerical Model, *Journal of Glaciology*, 27, 407–421, <https://doi.org/10.3189/S0022143000011448>, 1981.
- 815 Joughin, I., Smith, B., Howat, I., Scambos, T., and Moon, T.: Greenland flow variability from ice-sheet-wide velocity mapping, *J. Glaciol.*, 56, 415–430, <https://doi.org/10.3189/002214310792447734>, 2010.
- Joughin, I., Smith, B., Howat, I., and Scambos, T.: MEaSUREs Multi-year Greenland Ice Sheet Velocity Mosaic, Version 1. Boulder, Colorado USA. NASA National Snow and Ice Data Center Distributed Active Archive Center., <https://doi.org/10.5067/QUA5Q9SVMSJG.>, 2016.
- 820 Joughin, I., Smith, B., and Howat, I.: A complete map of Greenland ice velocity derived from satellite data collected over 20 years, *Journal of Glaciology*, 64, 1–11, <https://doi.org/10.1017/jog.2017.73>, 2018.
- Joughin, I., Smith, B. E., and Schoof, C. G.: Regularized Coulomb Friction Laws for Ice Sheet Sliding: Application to Pine Island Glacier, Antarctica, *Geophysical Research Letters*, 46, 4764–4771, <https://doi.org/10.1029/2019GL082526>, 2019.
- Larour, E., Seroussi, H., Morlighem, M., and Rignot, E.: Continental scale, high order, high spatial resolution, ice sheet modeling using the
- 825 Ice Sheet System Model (ISSM), *J. Geophys. Res. Earth Surf.*, 117, F01 022, <https://doi.org/10.1029/2011JF002140>, 2012.
- Leguy, G. R., Asay-Davis, X. S., and Lipscomb, W. H.: Parameterization of basal friction near grounding lines in a one-dimensional ice sheet model, *The Cryosphere*, 8, 1239–1259, <https://doi.org/10.5194/tc-8-1239-2014>, 2014.
- Lliboutry, L. and Duval, P.: Various isotropic and anisotropic ices found in glaciers and polar ice caps and their corresponding rheologies, *Ann. Geophys.*, 3, 207–224, 1985.

- 830 Minchew, B. M., Meyer, C. R., Pegler, S. S., Lipovsky, B. P., Rempel, A. W., Gudmundsson, G. H., and Iverson, N. R.: Comment on “Friction at the bed does not control fast glacier flow”, *Science*, 363, <https://doi.org/10.1126/science.aau6055>, 2019.
- Moon, T., Joughin, I., Smith, B., and Howat, I.: 21st-Century Evolution of Greenland Outlet Glacier Velocities, *Science*, 336, 576–578, <https://doi.org/10.1126/science.1219985>, 2012.
- Morlighem, M., Rignot, E., Seroussi, H., Larour, E., Dhia, H. B., and Aubry, D.: Spatial patterns of basal drag inferred using control methods from a full-Stokes and simpler models for Pine Island Glacier, West Antarctica, *Geophysical Research Letters*, 37, <https://doi.org/10.1029/2010GL043853>, 2010.
- 835 Morlighem, M., Williams, C. N., Rignot, E., An, L., Arndt, J. E., Bamber, J. L., Catania, G., Chauché, N., Dowdeswell, J. A., Dorschel, B., Fenty, I., Hogan, K., Howat, I., Hubbard, A., Jakobsson, M., Jordan, T. M., Kjeldsen, K. K., Millan, R., Mayer, L., Mouginot, J., Noël, B. P. Y., O’Cofaigh, C., Palmer, S., Rysgaard, S., Seroussi, H., Siegert, M. J., Slabon, P., Straneo, F., van den Broeke, M. R., Weinrebe, W.,
- 840 Wood, M., and Zinglensen, K. B.: BedMachine v3: Complete bed topography and ocean bathymetry mapping of Greenland from multi-beam echo sounding combined with mass conservation, *Geophys. Res. Lett.*, 44, 11 051–11 061, <https://doi.org/10.1002/2017GL074954>, 2017.
- Moss, R. H., Edmonds, J. A., Hibbard, K. A., Manning, M. R., Rose, S. K., van Vuuren, D. P., Carter, T. R., Emori, S., Kainuma, M., Kram, T., Meehl, G. A., Mitchell, J. F. B., Nakicenovic, N., Riahi, K., Smith, S. J., Stouffer, R. J., Thomson, A. M., Weyant, J. P., and Wilbanks, T. J.:
- 845 The next generation of scenarios for climate change research and assessment, *Nature*, 463, 747–756, <https://doi.org/10.1038/nature08823>, 2010.
- Mouginot, J., Rignot, E., Björk, A. A., van den Broeke, M., Millan, R., Morlighem, M., Noël, B., Scheuchl, B., and Wood, M.: Forty-six years of Greenland Ice Sheet mass balance from 1972 to 2018, *Proceedings of the National Academy of Sciences*, 116, 9239–9244, <https://doi.org/10.1073/pnas.1904242116>, 2019.
- 850 Nerem, R. S., Beckley, B. D., Fasullo, J. T., Hamlington, B. D., Masters, D., and Mitchum, G. T.: Climate-change-driven accelerated sea-level rise detected in the altimeter era, *P. Natl. Acad. Sci.*, 115, 2022–2025, <https://doi.org/10.1073/pnas.1717312115>, 2018.
- Noël, B., van de Berg, W. J., van Wessem, J. M., van Meijgaard, E., van As, D., Lenaerts, J. T. M., Lhermitte, S., Kuipers Munneke, P., Smeets, C. J. P. P., van Ulft, L. H., van de Wal, R. S. W., and van den Broeke, M. R.: Modelling the climate and surface mass balance of polar ice sheets using RACMO2 – Part I: Greenland (1958–2016), *The Cryosphere*, 12, 811–831, <https://doi.org/10.5194/tc-12-811-2018>,
- 855 2018.
- Nowicki, S., Bindschadler, R. A., Abe-Ouchi, A., Aschwanden, A., Bueller, E., Choi, H., Fastook, J., Granzow, G., Greve, R., Gutowski, G., Herzfeld, U., Jackson, C., Johnson, J., Khroulev, C., Larour, E., Levermann, A., Lipscomb, W. H., Martin, M. A., Morlighem, M., Parizek, B. R., Pollard, D., Price, S. F., Ren, D., Rignot, E., Saito, F., Sato, T., Seddik, H., Seroussi, H., Takahashi, K., Walker, R., and Wang, W. L.: Insights into spatial sensitivities of ice mass response to environmental change from the SeaRISE ice sheet modeling project II:
- 860 Greenland, *J. Geophys. Res. Earth Surf.*, 118, 1025–1044, <https://doi.org/10.1002/jgrf.20076>, 2013.
- Nowicki, S., Payne, A. J., Abe-Ouchi, A., Agosta, C., Alexander, P., Albrecht, T., Asay-Davis, X., Barthel, A., Calov, R., Chambers, C., Choi, Y., Cullather, R., Cuzzone, J., Dumas, C., Edwards, T., Felikson, D., Fettweis, X., Goelzer, H., Gladstone, R., Gолledge, N. R., Gregory, J. M., Greve, R., Hatterman, T., Hoffman, M. J., Humbert, A., Huybrechts, P., Jourdain, N. C., Kleiner, T., Larour, E., Le clec’h, S., Lee, V., Leguy, G., Lipscomb, W. H., Little, C. M., Lowry, D. P., Morlighem, M., Nias, I., Pattyn, F., Pelle, T., Price, S., Quiquet, A.,
- 865 Reese, R., Rückamp, M., Schlegel, N.-J., Seroussi, H., Shepherd, A., Simon, E., Slater, D., Smith, R., Straneo, F., Sun, S., Tarasov, L., Trusel, L. D., Breedam, J. V., van de Wal, R., van den Broeke, M., Winkelmann, R., Zhao, C., Zhang, T., and Zwinger, T.: Contrasting

- contributions to future sea level under CMIP5 and CMIP6 scenarios from the Greenland and Antarctic ice sheets, *Geophysical Research Letters*, submitted, 2020a.
- 870 Nowicki, S., Payne, A. J., Goelzer, H., Seroussi, H., Lipscomb, W. H., Abe-Ouchi, A., Agosta, C., Alexander, P., Asay-Davis, X. S., Barthel, A., Bracegirdle, T. J., Cullather, R., Felikson, D., Fettweis, X., Gregory, J., Hatterman, T., Jourdain, N. C., Kuipers Munneke, P., Larour, E., Little, C. M., Morlinghem, M., Nias, I., Shepherd, A., Simon, E., Slater, D., Smith, R., Straneo, F., Trusel, L. D., van den Broeke, M. R., and van de Wal, R.: Experimental protocol for sealevel projections from ISMIP6 standalone ice sheet models, *The Cryosphere Discussions*, 2020, 1–40, <https://doi.org/10.5194/tc-2019-322>, 2020b.
- 875 Nowicki, S. M. J., Payne, A., Larour, E., Seroussi, H., Goelzer, H., Lipscomb, W., Gregory, J., Abe-Ouchi, A., and Shepherd, A.: Ice Sheet Model Intercomparison Project (ISMIP6) contribution to CMIP6, *Geoscientific Model Development*, 9, 4521–4545, <https://doi.org/10.5194/gmd-9-4521-2016>, 2016.
- Pattyn, F.: A new three-dimensional higher-order thermomechanical ice-sheet model: basic sensitivity, ice-stream development and ice flow across subglacial lakes, *J. Geophys. Res. Solid Earth*, 108, 2382, <https://doi.org/10.1029/2002JB002329>, 2003.
- Pattyn, F. and Durand, G.: Why marine ice sheet model predictions may diverge in estimating future sea level rise, *Geophysical Research Letters*, 40, 4316–4320, <https://doi.org/10.1002/grl.50824>, 2013.
- 880 Pattyn, F., Perichon, L., Aschwanden, A., Breuer, B., de Smedt, B., Gagliardini, O., Gudmundsson, G. H., Hindmarsh, R. C. A., Hubbard, A., Johnson, J. V., Kleiner, T., Kononov, Y., Martin, C., Payne, A. J., Pollard, D., Price, S., Rückamp, M., Saito, F., Souček, O., Sugiyama, S., and Zwinger, T.: Benchmark experiments for higher-order and full-Stokes ice sheet models (ISMIP-HOM), *Cryosphere*, 2, 95–108, <https://doi.org/10.5194/tc-2-95-2008>, 2008.
- 885 Perego, M., Price, S., and Stadler, G.: Optimal initial conditions for coupling ice sheet models to Earth system models, *Journal of Geophysical Research: Earth Surface*, 119, 1894–1917, <https://doi.org/10.1002/2014JF003181>, 2014.
- Price, S. F., Payne, A. J., Howat, I. M., and Smith, B. E.: Committed sea-level rise for the next century from Greenland ice sheet dynamics during the past decade, *Proceedings of the National Academy of Sciences*, 108, 8978–8983, <https://doi.org/10.1073/pnas.1017313108>, 2011.
- 890 Rietbroek, R., Brunnabend, S.-E., Kusche, J., Schröter, J., and Dahle, C.: Revisiting the contemporary sea-level budget on global and regional scales, *P. Natl. Acad. Sci.*, 113, 1504–1509, <https://doi.org/10.1073/pnas.1519132113>, 2016.
- Rückamp, M., Falk, U., Frieler, K., Lange, S., and Humbert, A.: The effect of overshooting 1.5 °C global warming on the mass loss of the Greenland Ice Sheet, *Earth System Dynamics*, 9, 1169–1189, <https://doi.org/10.5194/esd-9-1169-2018>, 2018.
- Rückamp, M., Greve, R., and Humbert, A.: Comparative simulations of the evolution of the Greenland ice sheet under simplified Paris Agreement scenarios with the models SICOPOLIS and ISSM, *Polar Science*, 21, 14–25, <https://doi.org/10.1016/j.polar.2018.12.003>, 2019a.
- 895 Rückamp, M., Neckel, N., Berger, S., Helm, V., and Humbert, A.: Calving induced Speedup of Petermann Glacier, *Journal of Geophysical Research: Earth Surface*, 124, 216–228, <https://doi.org/10.1029/2018JF004775>, 2019b.
- Schoof, C.: The effect of cavitation on glacier sliding, *Proceedings of the Royal Society A*, pp. 609–627, <https://doi.org/10.1098/rspa.2004.1350>, 2005.
- 900 Seroussi, H. and Morlighem, M.: Representation of basal melting at the grounding line in ice flow models, *Cryosphere*, 12, 3085–3096, <https://doi.org/10.5194/tc-12-3085-2018>, 2018.
- Seroussi, H., Morlighem, M., Rignot, E., Khazendar, A., Larour, E., and Mouginot, J.: Dependence of century-scale projections of the Greenland ice sheet on its thermal regime, *J. Glaciol.*, 59, 1024–1034, <https://doi.org/doi:10.3189/2013JoG13J054>, 2013.

- 905 Seroussi, H., Morlighem, M., Larour, E., Rignot, E., and Khazendar, A.: Hydrostatic grounding line parameterization in ice sheet models, *Cryosphere*, 8, 2075–2087, <https://doi.org/10.5194/tc-8-2075-2014>, 2014.
- Shepherd, A., Ivins, E., Rignot, E., Smith, B., van den Broeke, M., Velicogna, I., Whitehouse, P., Briggs, K., Joughin, I., Krinner, G., Nowicki, S., Payne, T., Scambos, T., Schlegel, N., Geruo, A., Agosta, C., Ahlstrøm, A., Babonis, G., Barletta, V. R., Bjørk, A. A., Blazquez, A., Bonin, J., Colgan, W., Csatho, B., Cullather, R., Engdahl, M. E., Felikson, D., Fettweis, X., Forsberg, R., Hogg, A. E., Gallee, H., Gardner, A., Gilbert, L., Gourmelen, N., Groh, A., Gunter, B., Hanna, E., Harig, C., Helm, V., Horvath, A., Horwath, M., Khan, S., Kjeldsen, K. K., Konrad, H., Langen, P. L., Lecavalier, B., Loomis, B., Luthcke, S., McMillan, M., Melini, D., Mernild, S., Mohajerani, Y., Moore, P., Mottram, R., Mouginot, J., Moyano, G., Muir, A., Nagler, T., Nield, G., Nilsson, J., Noël, B., Ootosaka, I., Pattle, M. E., Peltier, W. R., Pie, N., Rietbroek, R., Rott, H., Sørensen, L. S., Sasgen, I., Save, H., Scheuchl, B., Schrama, E., Schröder, L., Seo, K.-W., Simonsen, S. B., Slater, T., Spada, G., Sutterley, T., Talpe, M., Tarasov, L., Jan van de Berg, W., van der Wal, W., van Wessem, M., Vishwakarma, B. D., Wiese, D., Wilton, D., Wagner, T., Wouters, B., Wuite, J., and Team, T. I.: Mass balance of the Greenland Ice Sheet from 1992 to 2018, *Nature*, <https://doi.org/10.1038/s41586-019-1855-2>, 2019.
- 910 Slater, D. A., Straneo, F., Felikson, D., Little, C. M., Goelzer, H., Fettweis, X., and Holte, J.: Estimating Greenland tidewater glacier retreat driven by submarine melting, *The Cryosphere*, 13, 2489–2509, <https://doi.org/10.5194/tc-13-2489-2019>, 2019.
- Slater, D. A., Felikson, D., Straneo, F., Goelzer, H., Little, C. M., Morlighem, M., Fettweis, X., and Nowicki, S.: Twenty-first century ocean forcing of the Greenland ice sheet for modelling of sea level contribution, *The Cryosphere*, 14, 985–1008, <https://doi.org/10.5194/tc-14-985-2020>, 2020.
- Sommers, A., Rajaram, H., and Morlighem, M.: SHAKTI: Subglacial Hydrology and Kinetic, Transient Interactions v1.0, *Geoscientific Model Development*, 11, 2955–2974, <https://doi.org/10.5194/gmd-11-2955-2018>, <https://www.geosci-model-dev.net/11/2955/2018/>, 2018.
- 925 Stearns, L. A. and van der Veen, C. J.: Friction at the bed does not control fast glacier flow, *Science*, 361, 273–277, <https://doi.org/10.1126/science.aat2217>, 2018.
- Weertman, J.: On the Sliding of Glaciers, *Journal of Glaciology*, 3, 33–38, <https://doi.org/10.3189/S0022143000024709>, 1957.
- Werder, M. A., Hewitt, I. J., Schoof, C. G., and Flowers, G. E.: Modeling channelized and distributed subglacial drainage in two dimensions, *Journal of Geophysical Research: Earth Surface*, 118, 2140–2158, <https://doi.org/10.1002/jgrf.20146>, 2013.
- 930 Wilson, N., Straneo, F., and Heimbach, P.: Submarine melt rates and mass balance for Greenland’s remaining ice tongues, *Cryosphere*, 11, 2773–2782, <https://doi.org/10.5194/tc-11-2773-2017>, 2017.